Environment Canada | Environnement Canada

Water Management | Gestion des Eaux

Development of Three-Dimensional Numerical Models of the Great Lakes

T. J. Simons

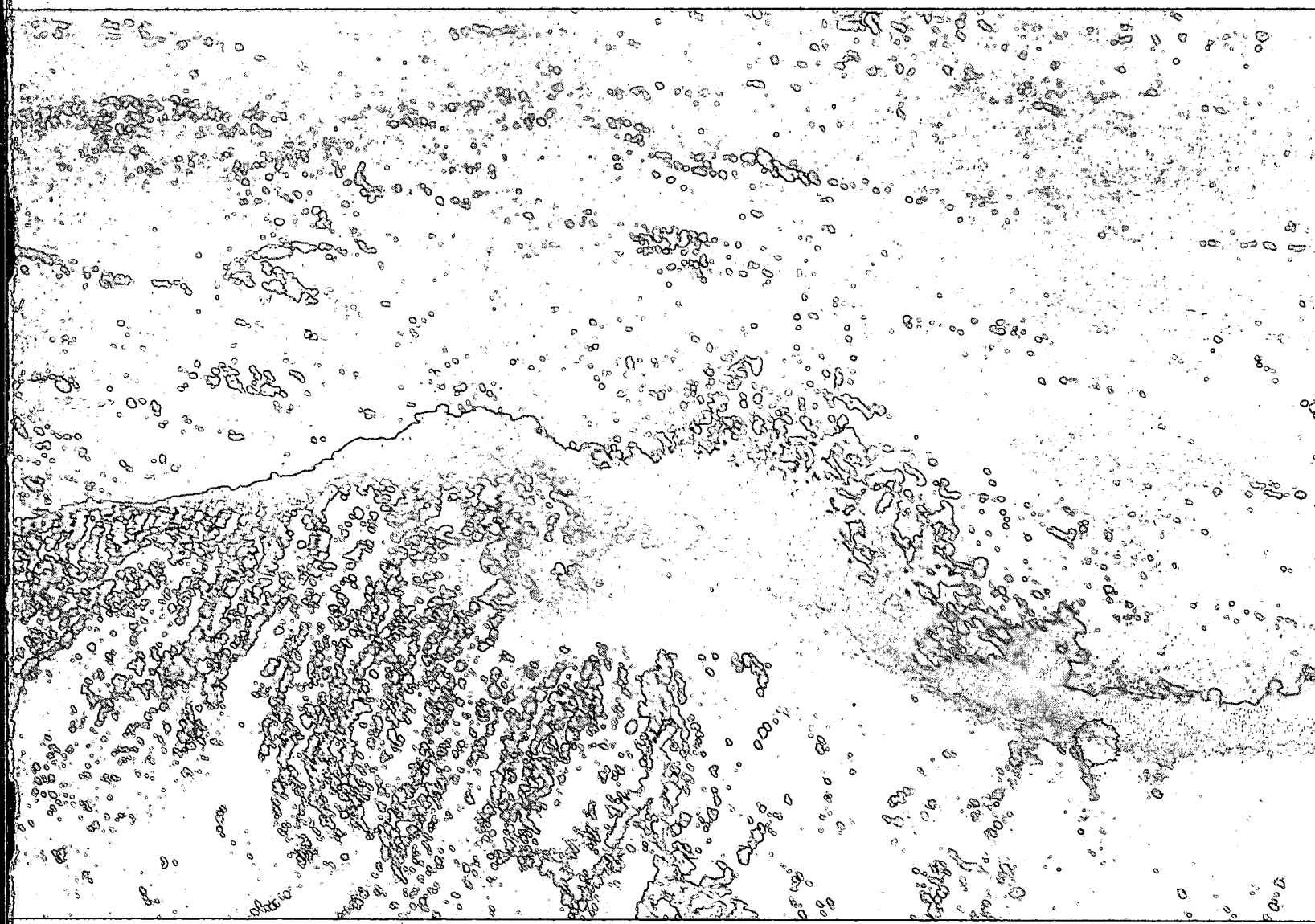

SCIENTIFIC SERIES NO. 12

INLAND WATERS DIRECTORATE,
CANADA CENTRE FOR INLAND WATERS,
BURLINGTON, ONTARIO, 1973.

Environment Canada | Environnement Canada
Water Management | Gestion des Eaux

Development of Three-Dimensional Numerical Models of the Great Lakes

T. J. Simons

SCIENTIFIC SERIES NO. 12

INLAND WATERS DIRECTORATE,
CANADA CENTRE FOR INLAND WATERS,
BURLINGTON, ONTARIO, 1973.

Cat.No.: En36-502/12

CONTRACT #02KXKL327-3-8060
THORN PRESS LIMITED

Contents

Illustrations

Tables

Abstract

This report describes a generalized numerical model for computing the water levels and the three-dimensional circulation and temperature structure of the Great Lakes. The mathematical-numerical framework is borrowed from numerical weather prediction, storm surge forecasting, and ocean circulation models. In view of the prominence of the boundary-value problem in the modeling of relatively shallow basins, emphasis is placed on the proper treatment of the bottom topography.

The model is based on the hydrostatic and the Boussinesq approximations and employs a quadratic relationship between temperature and density anomalies. The equations for the layered system are derived by vertical integration over layers and by defining new vertical velocities relative to the interfaces. Thereby the model allows for rigid horizontal levels, sloping permeable interfaces, moving material interfaces, or any combination of these.

The formulation of the finite-differencing scheme is based on considerations of the energy balance of the physical system, and accuracy and economy of numerical computations. The problems of grid dispersion and the treatment of lateral boundaries are investigated with the help of an exact solution obtained for the response of a lake to a time-dependent wind stress simulating the passage of an atmospheric front.

CHAPTER 1

Introduction

The numerical modeling of physical processes in the atmosphere and the oceans has advanced rapidly over the last two decades as a result of vast improvements in computing facilities. Such models are based on hydrodynamical and thermodynamical principles as expressed by appropriate mathematical equations. Although much insight has been gained from analytical solutions of these equations for certain idealized situations, a quantitative simulation of the highly complicated processes observed in nature can be attempted only by numerical methods. Indeed, these techniques have found important practical applications in the fields of numerical weather prediction and storm surge forecasting. The present problem, the modeling of the water motions in large lakes, is essentially of the same type and consequently a great amount of literature on modeling approximations and computational problems associated with such models is at our disposal.

In spite of their similarities, the various geophysical models differ widely in view of their individual objectives. The problem of computing the water circulation and temperature stratification of a lake is a boundary-initial value problem not unlike the problem of forecasting the weather. Thus the models require a specification of the boundary conditions including the shore configuration and depth contours together with the initial values of the flow parameters. However, much of the behaviour of the lake is a direct consequence of external forces such as wind stress and atmospheric pressure which tend to reduce the effects of the initial conditions. At the same time it has been well established that the mass circulation of a lake is mainly governed by the topography of the basin. This means that the boundary-value aspect of the present problem is more conspicuous than, for instance, in numerical weather prediction. Much research remains to be done on the numerical treatment of these boundaries.

The fundamental physical laws and corresponding mathematical equations governing the motions of lake waters and other physical parameters are known. Therefore in principle the problem facing us can be solved by numerical solution of the hydrodynamical differential equations, once certain numerical problems such as computational instability and truncation errors have been considered. However, the field of motions in a lake is in reality composed of scales of motions ranging all the way from the dimensions of the lake itself down to scales generally associated with turbulence. Thus, a straightforward numerical treatment of this complete range of scales cannot be attempted. In practice it is tacitly assumed that it is possible to model the large-scale organized motions without a detailed treatment of the smaller scale quasi-random turbulent motions. Unfortunately such separation of scales or spectral gap has not been well established and if it exists it is not clear at what scales it would occur. At present the best approach is to model a lake with increasing detail and investigate the solutions as a function of resolution. The interactions and the exchange of energy between the large-scale flow and the turbulent flow are then approximated by an appropriate parameterization of the small-scale phenomena.

From the foregoing it is clear that the modeling of the Great Lakes must proceed in distinct steps, starting from relatively simple models and advancing to fairly complicated models comparable to present-day atmospheric models (Phillips, 1959; Leith, 1965; Smagorinsky et al., 1965; Shuman and Hovermale, 1968). With regard to vertical resolution the first step is obviously the homogeneous model where the lake is represented by one layer of fluid of constant temperature and density. Such models have been used extensively to study the wind-driven ocean circulation and the storm-surge problem. In the first case the external gravity waves are generally filtered out but nonlinear effects are retained (Bryan, 1965; Veronis, 1966). A similar model by Paskausky (1969) has been applied to Lake Ontario. The second type of model is of course mainly concerned with the displacements of the free surface, and such effects as bottom friction, horizontal diffusion of momentum, and nonlinear inertial accelerations are generally discarded. Such storm surge models have been applied to the North Sea (Hansen, 1956; Fischer, 1959; Heaps, 1969), to the Great Lakes (Platzman, 1963; 1965), and to the Japanese seas (Miyazaki et al., 1961). Some recent models have combined the features of the ocean circulation and the storm-surge models (Ueno, 1965; Gates, 1968). These models constitute the basic framework for the homogeneous model described in the following.

Although such one-layer models may be useful for the prediction of storm surges and the study of the winter circulation of the lakes, they are subject to severe limitations. Thus, under homogeneous conditions, the vertical-mean flow as computed from the integrated models is indeed essentially correct, but this mean flow does not necessarily give an indication of the actual velocities to be found in the lake. In particular, the time variations of the

local currents bear hardly any relationship to the integrated volume transports. Certainly, a three-dimensional model becomes a necessity if one wants to study thermal effects and the interactions between the internal mass distributions and the water movements.

When considering this coupling of the thermodynamics and the hydrodynamics of the lakes, a distinction must be made between convection-type models and quasi-static models. The large-scale motions of a lake whose depth is much less than its horizontal dimensions, can be modeled as if the lake were always in a state of hydrostatic equilibrium. This assumption eliminates vertical accelerations due to buoyancy effects and it therefore precludes the explicit treatment of free convection associated with unstable stratifications. However, the assumption simplifies matters considerably and appears to be an appropriate principle for the present modeling program. Indeed, it is this hydrostatic approximation which has been applied with so much success in numerical weather prediction and in studies of the atmospheric circulation. Recently, essentially similar models have been used in oceanographic studies by Bryan and Cox (1967, 1968), Crowley (1968), Bryan (1969), and Cox (1970). The three-dimensional model presented in this report has been developed along similar lines, but more emphasis is placed on the treatment of the bottom topography which is of extreme importance for relatively shallow basins (e.g., Rao and Murty, 1970). Furthermore, the model is generalized to deal with various types of numerical representations in the vertical.

In principle, the numerical computations of the three-dimensional mass and velocity fields in a lake could employ a three-dimensional array of mesh-points. It is, however, more common among meterologists and oceanographers to visualize a three-dimensional model as a superposition of layers of fluid. The reasons for this are partly historical and partly physical in nature. For instance, during certain periods a lake may become stratified to the extent that apparent density discontinuities can be traced. This has led to the design of models consisting of layers of water of different densities and separated by moving material interfaces (Csanady, 1967, 1968a, 1968b; Yuen, 1968; Lee and Liggett, 1970; Welander, 1968). On the other hand, there are numerous occasions when a more or less continuous vertical density gradient exists. Such situations could be handled by a straightforward three-dimensional finite-difference grid, that is, a sequence of rigid permeable horizontal levels, which are employed in the three-dimensional ocean models referred to above. Or, it might be preferable to choose sloping instead of horizontal levels in dealing with lakes which generally show a gradual increase in depth from the shore to the interior.

With a view to allow for any one out of such a variety of models, the present three-dimensional model design employs the principles and the terminology of layered models, although the layers may be separated by rigid permeable interfaces instead of material surfaces. Thus, the equations for the layered system are obtained by vertical integration over each layer instead of applying the equations at given levels and replacing the vertical derivatives by finite differences. This procedure not only leads to greater versatility such as, for instance, a combination of moving and rigid interfaces in one and the same model, but in addition it may result in a more accurate model. At least, this procedure will ensure that certain volume integrals are preserved and consistency requirements are not violated.

In this regard it may be pointed out that we are dealing with relatively shallow bodies of water with large depth variations and relatively low vertical model resolution, which result in extreme horizontal variations of layer thicknesses over large regions. Since the bottom topography for such basins exerts a large effect on the water circulation, careful treatment of the depth variation is imperative. It is clear that a derivation of the model equations by integrating over the depth of each layer implies that the basin topography is identical for different vertical resolutions of the model and the equations for the layers can be added to give the vertically integrated model.

Other features of the three-dimensional model, in addition to those described above, are the following. The customary Boussinesq approximation is used so that the density variations are only allowed to enter in the buoyancy term, but the fluid is effectively incompressible. Thus, the vertical motion can be computed from the continuity of mass and the same equation can be used to predict the vertical displacements of the free surface and other substantial interfaces. The horizontal water displacements are computed from the so-called primitive equations, that is, the equations of motion in complete form, and the changes of temperature follow from the first law of thermodynamics. A quadratic relationship between the density anomaly and the temperature anomaly completes the set of equations.

In order to simulate sub-grid scale diffusion of momentum and heat, it is necessary to introduce eddy-viscosity coefficients and thermal diffusivities. In areas of unstable stratification, free convection is simulated by allowing the vertical diffusion of heat to be a function of static stability. Actually, as is common in numerical weather prediction, an infinitely large vertical flux of heat is invoked to counteract such instabilities. As is also common in meteorological models, the nonlinear terms are formulated on the basis of mass and energy conservations.

Since vertical displacements of the lake surface are not precluded, the model allows for external gravity waves. The speed of these waves is much greater than the internal wave speeds and consequently tends to put severe restrictions on the computational time step. Whereas the surface displacements may be of interest for other purposes, their effects on the internal mass distributions are unimportant. Thus, the internal structure of the flow may be computed in such a fashion that the effects of the free surface waves are

filtered out, which allows for a larger computational time step than the one used for the surface and mean flow prediction.

The present report consists of two major parts. Chapter 2 presents the equations for one-layer and multi-layered models, including the energy equations. Chapter 3 is devoted to a review of numerical techniques for space and time differentiation and an evaluation of the accuracy of our finite-difference schemes by comparison with solutions for idealized basins. Preliminary computations with a homogeneous and a four-layer stratified model of Lake Ontario have been reported by the author (Simons, 1971, 1972). The ultimate assessment of the degree of accuracy of a numerical model must be based on a comparison with observations carried out in the lakes. Pertinent observational data are expected to become available during the International Field Year on the Great Lakes planned for 1972. This will be an excellent opportunity to test the performance of the present models. A verification project of this type is planned and the results will be published under separate cover.

Equations for One-Layer and Multi-Layered Models

2.1 FUNDAMENTAL EQUATIONS

First, the customary Boussinesq approximation is introduced so that the variations of density are allowed to affect only the gravitational acceleration. The main simplification resulting from this approximation is that the water is effectively incompressible and thus the continuity equation reads

$$\frac{\partial u}{\partial x} + \frac{\partial v}{\partial y} + \frac{\partial w}{\partial z} = 0 \qquad (1)$$

where x and y are the horizontal coordinates positive to the east and to the north, respectively, z is the vertical coordinate positive upward from the mean water level, and u, v, and w, are the components of the velocity along the coordinates x, y, and z, respectively.

If equation (1) is integrated over a column of water extending from the bottom of the basin to the free surface, it clearly establishes a relationship between the change of surface level and the volume of water leaving or entering the column. This relationship can be obtained directly from considerations of mass conservation or can be derived from (1) by mathematical techniques. Thus if the depth of the lake is denoted by H, the free surface by ζ, and the time by t, then

$$\frac{\partial}{\partial x}\int_{-H}^{\zeta} u\,dz + \frac{\partial}{\partial y}\int_{-H}^{\zeta} v\,dz + \frac{\partial \zeta}{\partial t} = 0 \qquad (2)$$

The second assumption is that the large-scale water motions of relatively shallow basins can be modeled as if the water masses were always in hydrostatic equilibrium. The internal pressure distribution can then be obtained by vertical integration of the hydrostatic equation, the result of which may be written in the following form.

$$p = p_s + \rho_0 g(\zeta - z) + \int_z^{\zeta} \sigma\,dz \qquad (3)$$

where p is pressure, p_s is the atmospheric pressure at the air-sea interface, g is the gravitational acceleration of the earth, ρ is the density of water, ρ_0 is its value at the temperature of maximum density, and $\sigma \equiv (\rho - \rho_0)\,g$ is a measure of the density anomaly.

The density anomaly entering in (3) may be related to temperature and pressure by an equation of state. The variation of density anomaly at constant pressure is shown in Figure 1 against a linear temperature scale (solid curve) and also against a quadratic temperature scale (dashed curve). Since we are only concerned with horizontal pressure gradients the pressure effect can be ignored and to the order of the approximations made in the present model a sufficiently accurate equation of state is

$$\sigma = -\epsilon\,\theta^2; \quad \epsilon \text{ is constant} \qquad (4)$$

as indicated by the straight line in Figure 1. Here $\theta \equiv T - T_0$ is the deviation of the temperature from the temperature of maximum density. In principle, of course, any other equation of state can be employed.

For brevity of notation it is convenient to introduce the following definitions.

$$\psi \equiv p_s + \rho_0 g \zeta \qquad \phi \equiv \int_z^{\zeta} \sigma\,dz \qquad (5)$$

where ψ is a barotropic pressure function depending on the surface conditions only, and ϕ is the baroclinic pressure determined by the internal mass distributions. The latter varies with depth whereas the former is independent of the vertical coordinate. However, the barotropic pressure function is of course only part of the total barotropic pressure which in turn increases linearly with depth.

Next, two differential operators are defined to represent the advection of a scalar by large-scale motions on the one hand and the diffusion by sub-grid-scale fluxes on the other hand. Let φ represent any scalar depending on the time t and the space coordinates x, y, and z, and let α, β, and γ be the components of the diffusive-flux of this scalar along the coordinates x, y, and z, respectively. In the particular case of the flux of momentum the latter may be identified with the familiar Reynolds stresses. Now let

$$\mathcal{L}(\varphi) \equiv \frac{\partial \varphi}{\partial t} + \frac{\partial (u\varphi)}{\partial x} + \frac{\partial (v\varphi)}{\partial y} + \frac{\partial (w\varphi)}{\partial z}$$

$$\delta(\varphi) \equiv -\frac{\partial \alpha(\varphi)}{\partial x} - \frac{\partial \beta(\varphi)}{\partial y} - \frac{\partial \gamma(\varphi)}{\partial z} \qquad (6)$$

The first operator involving the divergence of the advective fluxes of the scalar φ can be shown to constitute the material time derivative of this scalar by virtue of the continuity equation (1). The second operator represents the three-dimensional diffusion and appears here as the convergence of the diffusive fluxes. The latter are related to the gradients of the function φ, but if φ is identified with

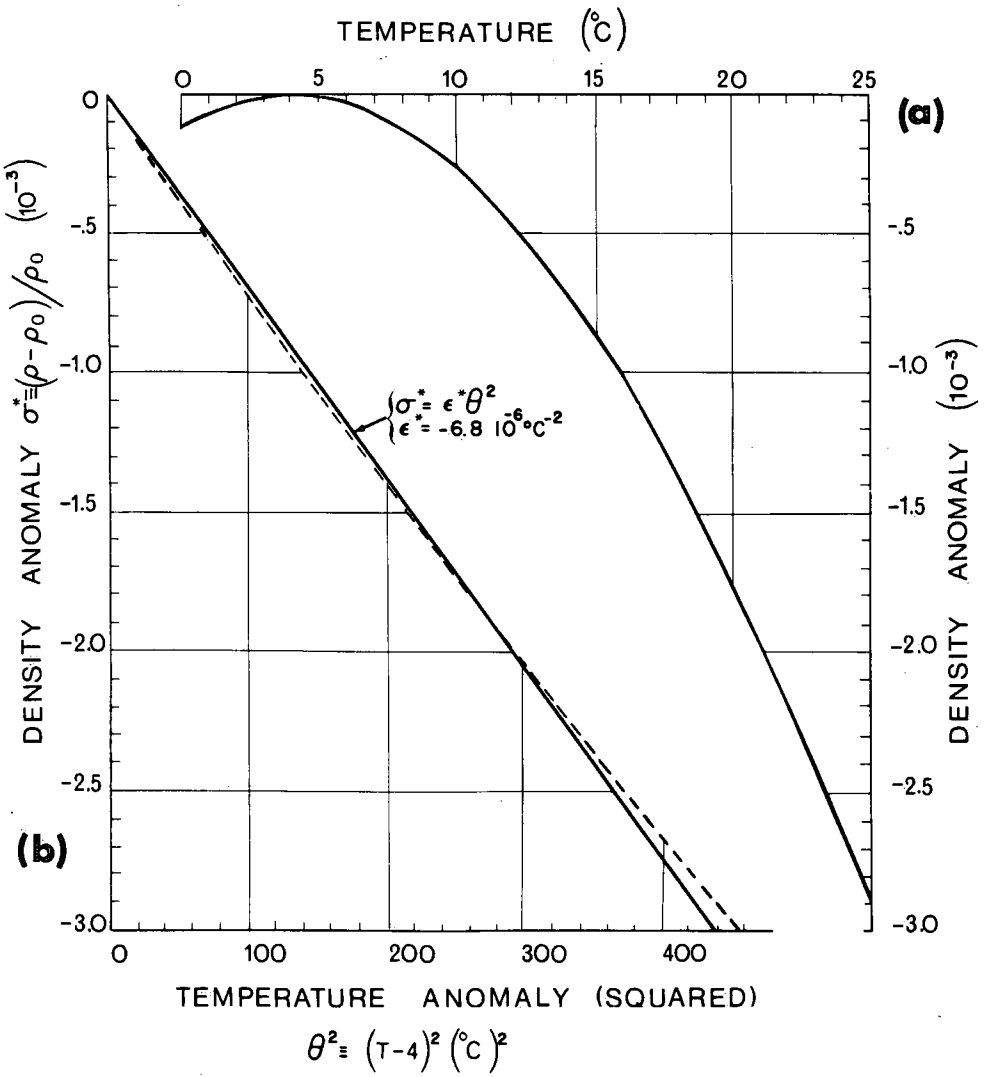

Figure 1. (a) density anomaly as a function of temperature at constant pressure; (b) density anomaly plotted against the squared temperature anomaly (dashed line) and approximation employed in the model (solid line).

one component of the velocity field, the fluxes are in general also dependent on the other velocity components.

Using (1) and (3), again neglecting the small density anomalies, and denoting the Coriolis parameter by f, the horizontal equations of motion may be written in the form

$$\mathcal{L}(u) = fv - \frac{\partial}{\partial x}\left(\frac{\psi + \phi}{\rho_0}\right) + \delta(u)$$
$$\mathcal{L}(v) = -fu - \frac{\partial}{\partial y}\left(\frac{\psi + \phi}{\rho_0}\right) + \delta(v) \qquad (7)$$

The temperature changes of the water masses are governed by the first law of thermodynamics with diabatic effects resulting from the three-dimensional eddy diffusion of heat. Assuming that the small compressibility effect can be neglected, the temperature equation may be written

$$\mathcal{L}(\theta) = \delta(\theta) \qquad (8)$$

where $\theta \equiv T - T_0$ is the temperature anomaly.

Although it is possible to proceed with the development of the layered models without specifying the diffusion relationships, a simple example will be presented here. The modeling of the diffusion of momentum has been discussed in some detail by Lilly (1967). For the moment it will be simply stipulated that the diffusive flux of momentum along a given coordinate be proportional to the gradient of the corresponding component of the large scale flow. Thus, if A and ν are the local coefficients of the horizontal and vertical eddy viscosity, the fluxes of the first

momentum component may be written

$$\alpha(u) = -A\frac{\partial u}{\partial x};\ \beta(u) = -A\frac{\partial u}{\partial y};\ \gamma(u) = -\nu\frac{\partial u}{\partial z} \qquad (9)$$

with similar expressions for the second velocity component. From (6) and (9) it follows that the horizontal fluxes combine to give a horizontal diffusion in the form of a Laplacian operator. In the numerical model this term will be interpreted in terms of sub-grid-scale diffusion, whereas the vertical flux component will appear in the form of stresses between layers of fluid, thus simulating the transfer of momentum from the surface downwards.

Similarly the horizontal diffusion and the vertical flux of heat are related to the temperature gradients

$$\alpha(\theta) = -A_\theta\frac{\partial \theta}{\partial x};\ \beta(\theta) = -A_\theta\frac{\partial \theta}{\partial y};\ \gamma(\theta) = -\kappa\frac{\partial \theta}{\partial z} \qquad (10)$$

where A_θ is the horizontal eddy diffusivity and κ is the vertical eddy diffusivity. The latter depends on the static stability $\partial\sigma/\partial z$ and is allowed to attain very large values for unstable situations in order to simulate the net effects of convective overturning. In practice this means that an instantaneous adjustment takes place to remove any static instability the moment it occurs in the model.

The equations above form a complete set and may be used to compute the evolution of the three-dimensional water circulation starting from given initial and boundary conditions. The primary boundary conditions are that the normal component of the velocity and the normal heat flux must vanish at a solid (insulated) boundary such as the shoreline and the bottom of the basin, whereas the flux of momentum normal to these boundaries must be specified by some stress condition. On the other hand, at a moving material surface such as the air-water interface, a water particle must follow the motion of that surface and the diffusive fluxes of heat and momentum through the interface are considered to be specified in terms of external parameters. With regard to the velocity components at the bottom and the free surface, the following conditions may be derived

$$\begin{aligned} z = \zeta: &\quad w = u\frac{\partial \zeta}{\partial x} + v\frac{\partial \zeta}{\partial y} + \frac{\partial \zeta}{\partial t} \\ z = -H: &\quad w = -u\frac{\partial H}{\partial x} - v\frac{\partial H}{\partial y} \end{aligned} \qquad (11)$$

The normal fluxes of momentum at the free surface and the bottom must equal the windstress τ_s and the bottom stress τ_b, respectively. Noting that the vertical fluxes are positive upward, whereas the stresses between layers are the forces exerted by the upper on the lower layer, the conditions for the first velocity component are

$$\begin{aligned} z = \zeta: &\quad \gamma(u) - \alpha(u)\frac{\partial \zeta}{\partial x} - \beta(u)\frac{\partial \zeta}{\partial y} = -\frac{\tau_{sx}}{\rho_0} \\ z = -H: &\quad \gamma(u) + \alpha(u)\frac{\partial H}{\partial x} + \beta(u)\frac{\partial H}{\partial y} = -\frac{\tau_{bx}}{\rho_0} \end{aligned} \qquad (12)$$

with similar conditions for the second component. Furthermore, if q_s is the downward surface flux of heat, then the conditions for the temperature flux normal to the boundaries can be written

$$\begin{aligned} z = \zeta: &\quad \gamma(\theta) - \alpha(\theta)\frac{\partial \zeta}{\partial x} - \beta(\theta)\frac{\partial \zeta}{\partial y} = -q_s \\ z = -H: &\quad \gamma(\theta) + \alpha(\theta)\frac{\partial H}{\partial x} + \beta(\theta)\frac{\partial H}{\partial y} = 0 \end{aligned} \qquad (13)$$

2.2 HOMOGENEOUS MODEL

In the process of developing an hierarchy of models describing the circulation of the Great Lakes, the first step is to consider the water transports under homogeneous conditions. Although the homogeneous model is just a special case of the more general multi-layered model described in the following section, it is worthwhile to discuss here the simplest homogeneous model, namely, the one-layer storm-surge model. This model is appropriate for a study of the basic circulation of the lakes during the colder part of the year and, from a computational viewpoint, it is useful for a systematic investigation of numerical techniques. In this case the vertical structure of the flow will not be considered and thus it is convenient to introduce the volume transport vector.

$$\mathbf{V} \equiv (U, V) \equiv \int_{-H}^{\zeta} \mathbf{v}\, dz \equiv \int_{-H}^{\zeta} (u, v)\, dz \qquad (14)$$

A measure of the water velocity is then obtained by averaging this volume transport over depth, thus

$$\bar{\mathbf{v}} \equiv (\bar{u}, \bar{v}) \equiv \frac{\mathbf{V}}{H+\zeta} \equiv \frac{(U, V)}{H+\zeta} \qquad (15)$$

In the present notation the continuity equation (2) becomes

$$\frac{\partial \zeta}{\partial t} = -\frac{\partial U}{\partial x} - \frac{\partial V}{\partial y} \qquad (16)$$

Since the model deals with a homogeneous body of water, the baroclinic pressure term does not appear in the equations of motion and hence the pressure terms of (7) become independent of depth. After substituting (6) into (7), the equations are integrated over the depth of the lake, whereby the terms of (6) are transformed by the rules for interchanging differentiation and integration and with the help of the boundary conditions (11-12). If further the horizontal eddy flux vector with components $\alpha(\phi)$ and $\beta(\phi)$ is denoted by $\Gamma(\phi)$, the integrated equations of motion become

$$\frac{\partial U}{\partial t} = -g\,(H+\zeta)\,\frac{\partial}{\partial x}\left(\zeta + \frac{p_s}{\rho g}\right) + fV + \tag{17}$$

$$+\frac{\tau_{sx} - \tau_{bx}}{\rho} - \nabla \int_{-H}^{\zeta} [\,\Gamma(u) + uv\,]dz$$

$$\frac{\partial V}{\partial t} = -g\,(H+\zeta)\,\frac{\partial}{\partial y}\left(\zeta + \frac{p_s}{\rho g}\right) - fU + \tag{18}$$

$$+\frac{\tau_{sy} - \tau_{by}}{\rho} - \nabla \int_{-H}^{\zeta} [\Gamma(v) + vv]\,dz$$

where the subscripts s and b attached to the stress components refer to the surface and bottom, respectively, ∇ is the horizontal gradient operator, and all other symbols have the same meaning as before. The last terms on the right represent the nonlinear inertial accelerations and originate from the left hand side of (7). A detailed discussion of the storm surge equations has been presented by Welander (1961).

At this point a number of approximations is introduced to obtain a closed system of equations. The nonlinear inertial terms are approximated as follows

$$\int_{-H}^{\zeta} u\,v\,dz = \frac{UV}{H+\zeta} \qquad \int_{-H}^{\zeta} v\,v\,dz = \frac{VV}{H+\zeta} \tag{19}$$

In reality, this vertical integration requires an assumption regarding the vertical velocity profiles and the approximation above applies essentially to the case of uniform velocity distribution in the vertical. Thus the approximation tends to underestimate the nonlinear effects and one might consider to multiply the results of the integrations above by a number larger than unity. In particular for a linear variation of velocity with depth the multiplicative factor would be 4/3. However, the approximation (19) seems adequate and will be introduced in the basic equations (17-18).

According to (6) and (9), the lateral diffusion of momentum has been assumed to be proportional to the Laplacian of the velocity field. It is possible of course to represent the horizontal viscosity effects in a more sophisticated manner but at present this seems hardly justified in view of our knowledge of the diffusion processes. The coefficient of lateral eddy diffusion is probably a function of the space coordinates. Its value is estimated for Lake Ontario to be of the order of $10^6\,cm^2/sec$. For comparison of numerical models of different horizontal resolution, the coefficient should be related in some fashion to the mesh size of the computational grid. Thus Ueno (1964) assumed A to be proportional to the 4/3th power of the grid distance over which the Laplacian is evaluated.

The vertical integration of the diffusion terms in equations (17-18) calls again for some assumption concerning the vertical profiles of the horizontal motions. Assuming the horizontal diffusion coefficient to be constant with depth, two different expressions for the eddy viscosity can be derived. If the velocities are assumed to be uniform with depth the vertical integrations of (9) can be performed immediately and the integrals become

$$\int_{-H}^{\zeta} \Gamma\,(u,v)\,dz = -A\,(H+\zeta)\,\nabla\,(\bar{u},\bar{v}) \tag{20}$$

On the other hand it may be more reasonable to realize that the water transports are concentrated in the upper layers of the lake and the deeper portions will contribute considerably less to the total transports. In that case a better approximation would be

$$\int_{-H}^{\zeta} \Gamma\,(u,v)\,dz = -A\,\nabla\,(U, V) \tag{21}$$

For the present calculations the latter form of the diffusion simulation has been adopted.

The bottom stresses must also be related to the volume transports in order to obtain a closed system of equations. The bottom friction can be made proportional to the velocity at the bottom as follows

$$\tau_b = \rho k |V_b| V_b$$

where k is a non-dimensional skin friction coefficient of the order of 2.5×10^{-3}. On assuming a uniform velocity distribution in the vertical, it follows then from (15) that

$$\frac{\tau_b}{\rho} = B\,V\,; \quad B \equiv \frac{k\,|V|}{(H+\zeta)^2} = \frac{k\,|\bar{v}|}{H+\zeta} \tag{22}$$

It is often convenient or at least more economical to linearize this expression in some fashion, assuming either typical mean velocities or typical volume transports. Computations with a Lake Ontario model show typical average velocities in shallow water of the order of 10 cm/sec as compared to velocities as low as 1 cm/sec in the deeper parts of the lake. The corresponding coefficient B would vary from 0.0025/H to 0.025/H cgs units and may be compared with the value B = 0.01/H cgs units adopted by Rao & Murty (1970). On the other hand, the mass transport field is much smoother than the mean velocity field and typical values are $2\text{-}4 \times 10^4\ cm^2/s$ for both the shallow and deep parts of the lake. Thus the bottom friction coefficient defined in (22) would vary between $B = 50/H^2$ and $B = 100/H^2$ cgs units.

Another expression for the bottom stress may be deduced from a solution of Ekman's problem where the vertical turbulent diffusion of momentum is prescribed by means of a constant eddy-viscosity coefficient ν. Thus Platzman (1963) derived a bottom friction coefficient as a function of the Ekman number $H\sqrt{f/2\nu}$ so that B approaches zero for large depths and tends to $B = 2.5\,\nu/H^2$

for shallow water. For Lake Erie, Platzman estimated ν = 40 cm^2/s which may be considered a reasonable value for the shallower parts of the Great Lakes where the bottom friction is most prominent. Thus one would again obtain for shallow water $B = 100/H^2$ cgs units. In summary, the alternatives for the bottom friction as defined in (22) are the following

(1) Linear $B = a/H$ $a \simeq 0.01$ cm/sec;

(2) Quasi-linear: $B = b/H^2$ $b \simeq 100\ cm^2/sec$; **(23)**

(3) Nonlinear: $B = k\,|V|\,/H^2$ $k \simeq 0.0025$,

where the surface elevation ζ has been neglected by comparison with the depth H.

The nonlinear bottom friction was used by Hansen (1956) in his pioneering work on the North Sea storm surges. Fischer (1959) used the quasi-linear formulation and Jelesnianski (1967) adopted Platzman's (1963) formulation. It may be noted here that the complete Ekman procedure implies a reduction of the pressure gradient by a factor 5/6 and an increase of the wind stress by a factor 1.25 for shallow parts of the lake. A slight rotation of the pressure gradient force and the bottom stress are also involved. Ueno (1964) adopted the nonlinear bottom friction but increased the wind stress by the factor 1.25. Jelesnianski (1970) subsequently derived an integral operator for the bottom stress that incorporates the time history of forces in the system in the form of a convolution integral implying a time lag between wind stress or surface slope and consequent bottom stress. However, for the present preliminary calculations only the three alternatives defined in (23) are compared.

The last terms of the equations (17-18) to be discussed are the external forces, i.e., the surface pressure and the wind stress. For the present calculations the surface pressure is set equal to zero since it can be incorporated in a straightforward manner in operational runs. The surface wind stress is customarily related to the wind velocity as follows

$$\tau_s = k\,\rho_a\,|V_a|V_a \qquad (24)$$

where ρ_a is the density of air ($1.2\ 10^{-3}$ cgs) and V_a is the wind velocity at anemometer level. The drag coefficient k has a nondimensional value of the order of 10^{-3} but its exact value is highly uncertain and depends, of course, on the surface parameters. In most studies of storm surges in the North Sea, the skin-friction coefficient was assigned values of the order of 3×10^{-3}; similar values were suggested by Platzman (1958a) and Ueno (1964). Recent observations indicate that an appropriate value for models of the Great Lakes might be as low as $k = 1.2 \times 10^{-3}$. This problem will not be considered here, since modeling approximations and numerical techniques rather than operational predictions are under discussion. Thus for the preliminary calculations, more or less typical windfields are used and in particular a scale value of the wind stress equal to $\tau_s / \rho = 1\ cm^2/s^2$ is assumed.

To complete the system of equations, the lateral boundary conditions must be specified. The first condition is that the component of velocity normal to the shore must tend to zero. Since the depth of the lake approaches zero at the shore the tangential component of the volume-transport vector will also tend to zero. However, this is equivalent to the condition of zero slip and therefore introduces an apparent friction. Nevertheless, this condition appears reasonable for the large-scale circulation and it is a proper boundary condition in conjunction with the horizontal eddy diffusion in Equations (17-18). The matter will be discussed in more detail in Chapter 3 with regard to the numerical treatment of the boundaries, and the effects of the boundary conditions on the large-scale flow will be evaluated in the latter part of Chapter 3.

2.3 MULTI-LAYERED MODEL

The layered model has been designed so that the equations for any vertical resolution are consistent with the vertically-integrated homogeneous model. This is ensured by integration of the continuity equation and the equations of motion over each layer of the model. Since the depth contours are among the most important factors determining the lake circulation, it is essential that the treatment of the bathymetry of the basin will not be adversely affected by the relatively low model resolution. Due to the large depth variations it is likely that the interfaces between the layers will intersect the bottom as shown in Figure 2. Therefore the number of layers will be a function of the horizontal coordinates and can be also time-dependent. For the ensuing mathematical development, and also for the purpose of the numerical computations by computer, it is more convenient to stipulate that the total number of layers be the same throughout the basin by letting an interface coincide with the bottom beyond their intersection. Thus formally each layer extends over the whole surface area of the basin.

Let K denote the number of layers and let h_k, k = 1, 2, . . . ,K−1, be the distance between the k-th interface and the equilibrium free surface (z=0). The character of the interfaces is not yet specified and the layers can be separated by moving material surfaces, h_k (t,x,y), rigid permeable interfaces, h_k (x,y), or rigid levels where h_k = constant. Thus it is convenient to denote the surfaces and the interfaces entering into the model by the general equation $z=Z_k$ (t,x,y), k=0,1, . . . , K. Recalling the notation for the surface deviation and the basin depth, the various interfaces are defined.

Free surface: $Z_0 = \zeta\,(t,x,y)$

Interfaces: $Z_k = -h_k\,(t,x,y)$, k=1,2, . . . , K−1 **(25)**

Bottom: $Z_K = -H\,(x,y)$

where for certain areas a number of the interfaces Z_k may coincide with the bottom Z_K as indicated in Figure 2.

The primary dependent variables are the layer thicknesses together with the velocity components and the temperature integrated over the depth of each layer. Thus the following parameters, which are functions of time and the horizontal coordinates, are introduced

$$\text{Layer thickness: } D_{k-\frac{1}{2}} \equiv Z_{k-1} - Z_k$$

$$\text{Layer transports: } (U,V)_{k-\frac{1}{2}} \equiv \int_{Z_k}^{Z_{k-1}} (u,v)\, dz \qquad (26)$$

$$\text{Layer "heat content": } T_{k-\frac{1}{2}} \equiv \int_{Z_k}^{Z_{k-1}} \theta\, dz$$

where k ranges from 1 to K. As indicated in Figure 2, a half-integer subscript refers to a layer whereas an integer subscript indicates a variable evaluated at an interface.

To simplify the notation for the generalized multi-layered model and the boundary conditions, a new vertical velocity relative to a surface Z_k is defined as follows

$$\omega_k \equiv w_k - u_k \frac{\partial Z_k}{\partial x} - v_k \frac{\partial Z_k}{\partial y} - \frac{\partial Z_k}{\partial t} \qquad (27)$$

and similarly the following measure of the diffusive flux through a surface Z_k is introduced

$$\chi(\varphi)_k \equiv \gamma(\varphi)_k - \alpha(\varphi)_k \frac{\partial Z_k}{\partial x} - \beta(\varphi)_k \frac{\partial Z_k}{\partial y} \qquad (28)$$

where α, β, and γ are the components of the sub-grid-scale flux of the scalar φ discussed earlier, and k ranges from 0 to K. If the scalar φ is identified with momentum and temperature, the flux parameter (28) may be considered to represent the stresses and the heat fluxes between layers, which in Figure 2 are indicated by the symbols τ and q, respectively.

Next, an advection and a diffusion operator corresponding to the definitions (6) may be defined for each layer

$$L(\varphi)_{k-\frac{1}{2}} \equiv \int_{Z_k}^{Z_{k-1}} \mathcal{L}(\varphi) dz \qquad \Delta(\varphi)_{k-\frac{1}{2}} \equiv \int_{Z_k}^{Z_{k-1}} \delta(\varphi) dz \qquad (29)$$

After integrating the terms of (6) over the depth of a layer, applying the rules for interchanging integration and differentiation, and using the definitions (27-28), the operators (29) take on the following form

$$\begin{aligned} L(\varphi)_{k-\frac{1}{2}} &\equiv \frac{\partial}{\partial t}\int_{Z_k}^{Z_{k-1}} \varphi dz + \frac{\partial}{\partial x}\int_{Z_k}^{Z_{k-1}} u\varphi dz + \frac{\partial}{\partial y}\int_{Z_k}^{Z_{k-1}} v\varphi dz \\ &\quad + (\omega\varphi)_{k-1} - (\omega\varphi)_k \\ \Delta(\varphi)_{k-\frac{1}{2}} &\equiv -\frac{\partial}{\partial x}\int_{Z_k}^{Z_{k-1}} \alpha(\varphi) dz - \frac{\partial}{\partial y}\int_{Z_k}^{Z_{k-1}} \beta(\varphi) dz \\ &\quad - \chi(\varphi)_{k-1} + \chi(\varphi)_k \end{aligned} \qquad (30)$$

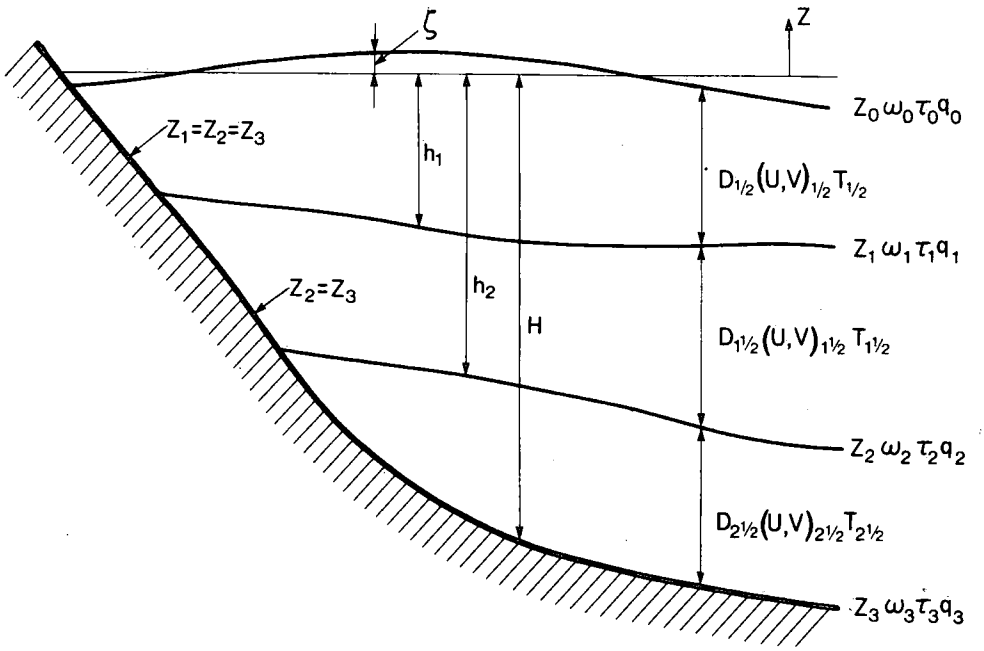

Figure 2. Vertical configuration of three-dimensional model.

The equations for computing the time rate of change of the layered variables (26) can now be derived from the basic equations (1), (7), and (8). First, integration of the continuity equation (1) and use of the definitions (26-27), results in

$$\frac{\partial D_{k-\frac{1}{2}}}{\partial t} + \frac{\partial U_{k-\frac{1}{2}}}{\partial x} + \frac{\partial V_{k-\frac{1}{2}}}{\partial y} + \omega_{k-1} - \omega_k = 0 \quad (31)$$

which, according to the first definition of (30), can be written formally as $L(1)_{k-\frac{1}{2}} = 0$. This equation makes it possible to compute either the displacement of a material surface ($\partial Z_k/\partial t$) or the apparent vertical motion through a rigid interface (ω_k). The computation starts with the bottom layer and proceeds upward through the model with the help of the following conditions which apply to the free surface, the bottom, and the two types of interfaces

$$\begin{aligned}
&\text{Free surface (impermeable) } Z_0 \text{ (t,x,y): } \omega_0 = 0 \\
&\text{Material interface (impermeable) } Z_k \text{ (t,x,y): } \omega_k = 0 \\
&\text{Rigid interface (permeable) } Z_k \text{ (x,y): } \frac{\partial Z_k}{\partial t} = 0 \\
&\text{Bottom (rigid, impermeable) } Z_K \text{ (x,y): } \omega_K = \frac{\partial Z_K}{\partial t} = 0
\end{aligned} \quad (32)$$

These conditions follow from the boundary conditions (11) and similar considerations for a material interface.

The equations of motion (7) integrated over the depth of a layer become

$$\begin{aligned}
L(u)_{k-\frac{1}{2}} &= fV_{k-\frac{1}{2}} - \frac{D_{k-\frac{1}{2}}}{\rho_0}\frac{\partial \psi}{\partial x} \\
&\quad - \int_{Z_k}^{Z_{k-1}} \frac{\partial}{\partial x}\left(\frac{\phi}{\rho_0}\right) dz + \Delta(u)_{k-\frac{1}{2}} \\
L(v)_{k-\frac{1}{2}} &= -fU_{k-\frac{1}{2}} - \frac{D_{k-\frac{1}{2}}}{\rho_0}\frac{\partial \psi}{\partial y} \\
&\quad - \int_{Z_k}^{Z_{k-1}} \frac{\partial}{\partial y}\left(\frac{\phi}{\rho_0}\right) dz + \Delta(v)_{k-\frac{1}{2}}
\end{aligned} \quad (33)$$

and the integrated thermal energy equation follows from (8).

$$L(\theta)_{k-\frac{1}{2}} = \Delta(\theta)_{k-\frac{1}{2}} \quad (34)$$

If it is assumed that the density varies slowly within each layer, the baroclinic pressure defined in (5) varies in a quasi-linear fashion within that layer. Differentiating the latter with respect to the horizontal coordinates and integrating over the layer depth then gives the result

$$\int_{Z_k}^{Z_{k-1}} \nabla\phi dz = D_{k-\frac{1}{2}} \nabla\phi_{k-\frac{1}{2}} + S_{k-\frac{1}{2}} \nabla Z_{k-\frac{1}{2}} \quad (35)$$

where the following definitions have been introduced

$$\begin{aligned}
Z_{k-\frac{1}{2}} &\equiv \frac{1}{2}(Z_{k-1} + Z_k) \\
S_{k-\frac{1}{2}} &\equiv \int_{Z_k}^{Z_{k-1}} \sigma\, dz \\
\phi_{k-\frac{1}{2}} &\equiv \int_{Z_{k-\frac{1}{2}}}^{\zeta} \sigma\, dz
\end{aligned} \quad (36)$$

The first term on the right of (35) is simply the gradient of the baroclinic pressure, as defined by (5), evaluated at the midpoint of a layer. The last term of (35) is a correction term to account for the variable thicknesses of the layers. The system of equations (31-36) is completed by recalling the definition of the barotropic pressure function (5), the equation of state (4) relating the density anomaly to the temperature, and the diffusion relationships (9-10).

For the purpose of numerical computations, the integrals defined by (30) and (36), the temperatures and the horizontal velocities at the interfaces, and the diffusion relationships must be expressed in terms of the primary dependent variables (26). A satisfactory approximation to the integrated product of two variables is of the following type

$$\int_{Z_k}^{Z_{k-1}} u\,\theta\, dz = \left(\frac{UT}{D}\right)_{k-\frac{1}{2}} \quad (37)$$

where the variables are defined by (26). Thus, in the event that the equation of state is of the form (4), the layer density defined in (36) becomes

$$S_{k-\frac{1}{2}} = -\epsilon\left(\frac{T^2}{D}\right)_{k-\frac{1}{2}} \quad (38)$$

and the advection of temperature follows from (30)

$$\begin{aligned}
L(\theta)_{k-\frac{1}{2}} &\equiv \frac{\partial T_{k-\frac{1}{2}}}{\partial t} + \frac{\partial}{\partial x}\left(\frac{UT}{D}\right)_{k-\frac{1}{2}} \\
&\quad + \frac{\partial}{\partial y}\left(\frac{VT}{D}\right)_{k-\frac{1}{2}} + (\omega\theta)_{k-1} - (\omega\theta)_k
\end{aligned} \quad (39)$$

The nonlinear inertial terms in the equations of motion will be approximated in the same way. As shown in the next section, the interpolation scheme to obtain the temperatures and the horizontal velocity components at the interfaces is dictated by energy considerations.

The horizontal diffusion, the interface stresses, and the temperature fluxes can be formulated in a number of ways.

A straightforward finite-difference expression for the vertical temperature flux defined by (10) is

$$\gamma(\theta)_k = -2\kappa \frac{(T/D)_{k-\frac{1}{2}} - (T/D)_{k+\frac{1}{2}}}{D_{k-\frac{1}{2}} + D_{k+\frac{1}{2}}} \quad (40)$$

If the vertical variation of the horizontal heat fluxes within a layer are neglected, the integrals entering in the diffusion operator (30) may be approximated as follows

$$\int_{Z_k}^{Z_{k-1}} \alpha(\theta)\, dz = -\left[A_\theta D \frac{\partial}{\partial x}\left(\frac{T}{D}\right)\right]_{k-\frac{1}{2}} \quad (41)$$

for the temperature flux defined by (10). Thus the diffusion of temperature is according to (30) described by the operator

$$\begin{aligned}\Delta(\theta)_{k-\frac{1}{2}} = &\frac{\partial}{\partial x}\left[A_\theta D \frac{\partial}{\partial x}\left(\frac{T}{D}\right)\right]_{k-\frac{1}{2}} \\ &+ \frac{\partial}{\partial y}\left[A_\theta D \frac{\partial}{\partial y}\left(\frac{T}{D}\right)\right]_{k-\frac{1}{2}} \\ &- \chi(\theta)_{k-1} + \chi(\theta)_k\end{aligned} \quad (42)$$

where the last terms are defined by (28). Similar expressions are used for the interface stresses and the horizontal diffusion of momentum.

The boundary conditions on the normal fluxes defined by (28) follow immediately from (12) and (13). Thus at the free surface and the bottom, respectively,

$$\begin{aligned}&\chi(u)_0 = -\frac{\tau_{sx}}{\rho_0}\ ;\ \chi(v)_0 = -\frac{\tau_{sy}}{\rho_0}\ ;\ \chi(\theta)_0 = -q_s. \\ &\chi(u)_K = -\frac{\tau_{bx}}{\rho_0}\ ;\ \chi(v)_K = -\frac{\tau_{by}}{\rho_0}\ ;\ \chi(\theta)_K = 0.\end{aligned} \quad (43)$$

The total heat content of the basin is conserved (in the absence of surface fluxes q_s) by the lateral boundary conditions

$$\frac{\partial}{\partial n}\left(\frac{T}{D}\right) = 0 \quad (44)$$

where n is the direction normal to the lake shore. The stresses at the bottom of the basin must be expressed in terms of the flow field, for example, by the relationship

$$\tau_b = \rho_0 k \,|\, V_b \,|\, V_b \quad (45)$$

where the bottom velocities may be approximated by the average velocities in the lowest layer.

If the wind stress and the temperature flux at the surface are known, then all the necessary equations to predict the evolution of the flow field from given initial conditions are available. Thus, starting from the temperature, the horizontal transport components, and the positions of all interfaces, including the air-water interface, the barotropic pressure gradient follows from (5), the baroclinic pressure gradient from (35), (36), and (38), and the vertical motion at rigid interfaces from (31). Then the time rate of change of the primary variables is governed by (31), (33) and (34). In principle, the latter equations are of the same type as the governing equations for the homogeneous model and, consequently, the same numerical techniques can be applied. The numerical methods will be discussed in Chapter 3.

2.4 ENERGY CONSIDERATIONS

The kinetic and the potential energy of a column of water extending from the bottom of the basin to the free surface are defined

$$\begin{aligned}&K \equiv \int_{-H}^{\zeta} k\, dz\ ;\ k \equiv \frac{1}{2}\rho_0 (u^2 + v^2) \\ &P \equiv \int_{-H}^{\zeta} \rho g z\, dz = \frac{1}{2}\rho_0 g (\zeta^2 - H^2) + \int_{-H}^{\zeta} \sigma z dz\end{aligned} \quad (46)$$

To derive expressions for the time rate of change of these energy quantities, recourse must be taken to the fundamental equations (1–13). First it may be noted that the operator (6) represents essentially the so-called substantial or material time derivative and consequently the following identities hold

$$\begin{aligned}&\mathcal{L}(\varphi^2) = 2\varphi \mathcal{L}(\varphi) \\ &\mathcal{L}(\varphi z) = \varphi w + z\mathcal{L}(\varphi)\end{aligned} \quad (47)$$

which can be verified also by partial differentiation of (6) and substitution of (1). If the equation of state is of the form (4), then it follows from (46) and (47) that

$$\begin{aligned}&\mathcal{L}(k) = \rho_0 u \mathcal{L}(u) + \rho_0 v \mathcal{L}(v) \\ &\mathcal{L}(\sigma z) = \sigma w - 2\epsilon z \theta \mathcal{L}(\theta)\end{aligned} \quad (48)$$

Now substituting the equations of motion (7) and the thermal energy equation (8) into the right-hand sides of (48) gives

$$\begin{aligned}&\mathcal{L}(k) = -u\frac{\partial}{\partial x}(\rho_0 g \zeta + \phi) - v\frac{\partial}{\partial y}(\rho_0 g \zeta + \phi) + G \\ &\mathcal{L}(\sigma z) = \sigma w + Q\end{aligned} \quad (49)$$

where

$$\begin{aligned}&G \equiv u\left[\rho_0 \delta(u) - \frac{\partial p_s}{\partial x}\right] + v\left[\rho_0 \delta(v) - \frac{\partial p_s}{\partial y}\right] \\ &Q \equiv -2\epsilon z \theta \mathcal{L}(\theta) = -2\epsilon z \theta \delta(\theta)\end{aligned} \quad (50)$$

The latter represent the effects of diffusion, dissipation, and external agents. It will be shown that in the absence of these terms the sum of the total kinetic and potential energy for the basin is conserved. Subsequently, similar relationships will be derived for the layered model.

First it may be verified by partial differentiation and by using (1) that the first of expressions (49) is equivalent to

$$\mathcal{L}(k+\phi+\rho_0 g\zeta) = \frac{\partial}{\partial t}(\phi+\rho_0 g\zeta) + w\frac{\partial \phi}{\partial z} + G \qquad (51)$$

Secondly, by integrating (6) in the vertical, using the rules for interchanging differentiation and integration, and applying the boundary conditions (11), it is found that

$$\int_{-H}^{\zeta} \mathcal{L}(\varphi)dz = \frac{\partial}{\partial t}\int_{-H}^{\zeta} \varphi dz + \frac{\partial}{\partial x}\int_{-H}^{\zeta} u\varphi dz + \frac{\partial}{\partial y}\int_{-H}^{\zeta} v\varphi dz \qquad (52)$$

and also, since (5) implies that $\phi = 0$ at the free surface,

$$\frac{\partial}{\partial t}\int_{-H}^{\zeta}(\phi+\rho_0 g\zeta)\,dz = \int_{-H}^{\zeta}\frac{\partial}{\partial t}(\phi+\rho_0 g\zeta)\,dz + \rho_0 g\zeta\frac{\partial \zeta}{\partial t} \qquad (53)$$

Thus, integrating (51) over the total depth, using (52-53) and the first definition of (46), results in

$$\frac{\partial K}{\partial t} = -\frac{\partial}{\partial x}\int_{-H}^{\zeta} u(k+\phi+\rho_0 g\zeta)dz - \frac{\partial}{\partial y}\int_{-H}^{\zeta} v(k+\phi+\rho_0 g\zeta)dz - \rho_0 g\zeta\frac{\partial \zeta}{\partial t} + \int_{-H}^{\zeta}\left(w\frac{\partial \phi}{\partial z} + G\right)dz \qquad (54)$$

whereas from (46), (49), and (52) the following is arrived at

$$\frac{\partial P}{\partial t} = -\frac{\partial}{\partial x}\int_{-H}^{\zeta} u(\sigma z)\,dz - \frac{\partial}{\partial y}\int_{-H}^{\zeta} v(\sigma z)\,dz + \rho_0 g\zeta\frac{\partial \zeta}{\partial t} + \int_{-H}^{\zeta}(w\sigma + Q)\,dz \qquad (55)$$

According to (5), $\sigma = -\partial\phi/\partial z$ and consequently the third and the fourth terms on the right of (54) and (55) are equal in magnitude but of opposite sign (if the source-sink terms G and Q are excluded), representing conversions of potential to kinetic energy or vice versa. The first two terms integrate out over the whole area of the basin by virtue of the condition that the transport across the boundary must vanish.

Let us now consider the energy conversions in the layered model. The kinetic and the potential energy for a layer of water of unit horizontal area may be written as follows

$$K_{k-\frac{1}{2}} \equiv \int_{Z_k}^{Z_{k-1}} k dz = \frac{1}{2}\rho_0 (U^2_{k-\frac{1}{2}} + V^2_{k-\frac{1}{2}}) / D_{k-\frac{1}{2}}$$

$$P_{k-\frac{1}{2}} \equiv \int_{Z_k}^{Z_{k-1}} \rho g z dz = \frac{1}{2}\rho_0 g (Z^2_{k-1} - Z^2_k) + Z_{k-\frac{1}{2}} S_{k-\frac{1}{2}} \qquad (56)$$

where the layered variables are defined by (25), (26), (36), and (38). Now suppose that the temperature and the horizontal velocity components at an interface are approximated by an interpolation formula of the type

$$\theta_k \equiv \frac{1}{2}\left(\frac{T}{D}\right)_{k-\frac{1}{2}} + \frac{1}{2}\left(\frac{T}{D}\right)_{k+\frac{1}{2}} \qquad (57)$$

but that the quadratic expression for the density anomaly (4) at an interface is defined as follows

$$\sigma_k \equiv -\epsilon\left(\frac{T}{D}\right)_{k-\frac{1}{2}}\left(\frac{T}{D}\right)_{k+\frac{1}{2}} \qquad (58)$$

with a similar definition for the kinetic energy k at the interface. Then it can be verified from (39), with the help of (31), (38), the second of definitions (36), and the first of definitions (56), that the following identities hold

$$\rho_0\left[\frac{U}{D}L(u) + \frac{V}{D}L(v)\right]_{k-\frac{1}{2}} = L(k)_{k-\frac{1}{2}}$$
$$2\epsilon\left[\frac{T}{D}L(\theta)\right]_{k-\frac{1}{2}} = -L(\sigma)_{k-\frac{1}{2}} \qquad (59)$$

The above relationships essentially imply that the layered representation of the nonlinear terms does not introduce spurious energies. Thus, after summing the right hand sides of (59) over all layers, the vertical motion terms cancel one another as indeed they should. In the terminology of finite-difference schemes this layered model possesses a variance-conserving property as discussed by Arakawa (1966), Bryan (1966), and Lilly (1965).

The energy equations for a layer are obtained by relating the time rate of change of the energies (56) to the right hand sides of (59) by virtue of (39) and subsequently substituting the equations (33-34) into the left-hand sides of (59). If further the layered equivalents of (50) are defined

$$G_{k-\frac{1}{2}} \equiv - U_{k-\frac{1}{2}} \frac{\partial p_s}{\partial x} - V_{k-\frac{1}{2}} \frac{\partial p_s}{\partial y} + \rho_0 \left[\frac{U}{D} \Delta (u) + \frac{V}{D} \Delta (v) \right]_{k-\frac{1}{2}}$$

$$Q_{k-\frac{1}{2}} \equiv - 2\epsilon \left[\frac{ZT}{D} L(\theta) \right]_{k-\frac{1}{2}} = - 2\epsilon \left[\frac{ZT}{D} \Delta (\theta) \right]_{k-\frac{1}{2}} \quad (60)$$

then after a partial differentiation with respect to x and y and substitution of the continuity equation (31)

$$\frac{\partial K_{k-\frac{1}{2}}}{\partial t} = - \frac{\partial}{\partial x} \left[U \left(\frac{K}{D} + \phi + \rho_0 g \zeta \right) \right]_{k-\frac{1}{2}} - \frac{\partial}{\partial y} \left[V \left(\frac{K}{D} + \phi + \rho_0 g \zeta \right) \right]_{k-\frac{1}{2}} - \left(\frac{US}{D} \frac{\partial Z}{\partial x} + \frac{VS}{D} \frac{\partial Z}{\partial y} + \phi \frac{\partial D}{\partial t} \right)_{k-\frac{1}{2}} - \phi_{k-\frac{1}{2}} (\omega_{k-1} - \omega_k) - \rho_0 g \zeta \left(\frac{\partial D_{k-\frac{1}{2}}}{\partial t} + \omega_{k-1} - \omega_k \right) - (\omega k)_{k-1} - (\omega k)_k + G_{k-\frac{1}{2}} \quad (61)$$

$$\frac{\partial P_{k-\frac{1}{2}}}{\partial t} = - \frac{\partial}{\partial x} (UZS/D)_{k-\frac{1}{2}} - \frac{\partial}{\partial y} (VZS/D)_{k-\frac{1}{2}} + \left(\frac{US}{D} \frac{\partial Z}{\partial x} + \frac{VS}{D} \frac{\partial Z}{\partial y} + S \frac{\partial Z}{\partial t} \right)_{k-\frac{1}{2}} - Z_{k-\frac{1}{2}} \left[(\omega\sigma)_{k-1} - (\omega\sigma)_k \right] + \rho_0 g \left(Z_{k-1} \frac{\partial Z_{k-1}}{\partial t} - Z_k \frac{\partial Z_k}{\partial t} \right) + Q_{k-\frac{1}{2}} \quad (62)$$

If (61) and (62) are summed over all the layers and integrated over the area of the basin, then the right-hand sides of (61) and (62) should cancel each other except for the generation terms. It can be easily verified that this cancellation takes place if

$$\sum_{k=1}^{K} \phi_{k-\frac{1}{2}} \frac{\partial D_{k-\frac{1}{2}}}{\partial t} = \sum_{k=1}^{K} S_{k-\frac{1}{2}} \frac{\partial Z_{k-\frac{1}{2}}}{\partial t}$$

$$\sum_{k=1}^{K} \phi_{k-\frac{1}{2}} (\omega_{k-1} - \omega_k) = \sum_{k=1}^{K} Z_{k-\frac{1}{2}} \left[(\omega\sigma)_k - (\omega\sigma)_{k-1} \right] \quad (63)$$

For a layered system with impermeable material interfaces ($\omega_k = 0$) it is found from (26), (32), and (36) that the conditions (63) are satisfied if

$$\phi_{\frac{1}{2}} = \frac{1}{2} S_{\frac{1}{2}}$$

$$\phi_{k+\frac{1}{2}} - \phi_{k-\frac{1}{2}} = \frac{1}{2} (S_{k-\frac{1}{2}} + S_{k+\frac{1}{2}}) \quad (64)$$

On the other hand, at rigid permeable levels ($\partial Z_k / \partial t = 0$) (63) can be obviously satisfied by

$$\phi_{k+\frac{1}{2}} - \phi_{k-\frac{1}{2}} = \sigma_k (Z_{k-\frac{1}{2}} - Z_{k+\frac{1}{2}}) \quad (65)$$

The approximations (64) and (65) indeed represent two reasonable alternatives for the numerical integration of the baroclinic pressure at the mid-levels defined by (36). This seems true for only one of the other two formulas (57) and (58), which were introduced earlier in order to arrive at the present energy-conserving layered system. The interpolation formula (57) is not only acceptable from a viewpoint of accuracy, but also is essential to preserve the variance of the primary variables (26), as will be shown in Chapter 3. This formula is to be used for computing the temperature and the horizontal velocity components at an interface, thus assuring that the nonlinear terms in the equations (33) and (34) do not give rise to spurious energy. On the other hand, a question may be raised with regard to the accuracy of the formula (65), if the density at an interface, σ_k, is computed according to the definition (58). In this case it may be preferable to use a more accurate formula even if this results in a violation of the energy conservation rules. Although such modifications can be allowed in the operational runs of the model, the present formulation is certainly very useful for the purpose of testing the computer program.

CHAPTER 3

Numerical Techniques for Space and Time Differentiation

3.1 NUMERICAL TIME INTEGRATION

A great number of studies have been devoted to the numerical solution of equations of the present type in connection with the development of numerical weather prediction. Although most investigations have been concerned with the problems of space-differencing, interest in time-differencing procedures has recently increased as a consequence of improvements in space-differencing techniques and the application of spectral techniques. Actually, methods of time-extrapolation are well developed since the problem is essentially equivalent to the numerical solution of a system of ordinary first-order differential equations in time. The result is an abundance of numerical prediction schemes of various types such as explicit and implicit schemes, single-step and multi-step schemes. In choosing a particular forecasting scheme one must combine considerations of economy and accuracy. The latter depends to a large extent on the form of the equations and the character of the solutions, that is, the water motions to be studied.

In the absence of external forces and frictional effects, the major terms in the present equations are the pressure gradients and the divergence terms which together describe the propagation of gravity waves in the lake. Since the Coriolis terms also represent a wave motion it is clear that the effects of various time-extrapolation schemes on the solution of the wave equation should be considered. This problem has been investigated by Kurihara (1965). Subsequently Lilly (1965), Young (1968), and Baer and Simons (1970) included the treatment of the nonlinear inertial terms. From these and other studies it is known that many forecasting schemes have filtering properties which may be desirable for specific purposes. However, based on considerations of accuracy, stability, and economy, it appears that for wave motions none of the schemes proposed to date is substantially superior to the familiar method of centered time differences often referred to as the mid-point rule, the step-over, or the leapfrog method. The computational mode associated with this scheme may cause a time-splitting of the solution into quasi-independent solutions for even and odd time steps but this can be suppressed by a half-time-step starting procedure (see e.g., Baer and Simons, 1970), or by a re-start, or by a time-smoothing at regular time intervals (Smagorinsky et al., 1965).

The mid-point rule is computationally neutral in the sense that the amplitudes of oscillatory solutions are preserved if the time step is small enough to satisfy the stability criterion. When combined with centered differences in the space domain the stability criterion is the familiar Courant-Friedrichs-Lewy condition for hyperbolic equations. Thus, if the centered differences are evaluated over $2\Delta t$ and $2\Delta s$ in time and space, respectively, then computational stability is assured if

$$\frac{\Delta t}{\Delta s} < \frac{1/\sqrt{2}}{C_{max}} \qquad (66)$$

where C_{max} is the speed of propagation of the fastest waves in the model, and therefore equal to $\sqrt{gH}$, that is, the speed of external gravity waves, in the present model.

While the centered time-differencing procedure is computationally neutral for our equations in the absence of bottom friction and diffusion, the same scheme is computationally unstable for dissipation terms. As noted by Platzman (1963) the dissipation terms represent a motion of pure decay described by a first order equation in time, whereas wave motion is described by an equation with second order time derivatives. On the other hand, single-step forward differencing results in amplification of oscillatory solutions but is stable for dissipative terms for small enough time steps. Thus an appropriate time extrapolation scheme for the present equations is one where the pressure gradient terms, the divergence terms, the Coriolis terms, and the non-linear terms are evaluated at a time-step centered between the old and new time, while the dissipation and diffusion terms are evaluated at the old time step. The computational stability condition for the complete equations will be more restrictive than the condition (66) but the latter is a satisfactory indicator of the time step to be used in the integration. In the final analysis the stability of the calculation must be judged by monitoring certain conservative parameters such as total energy in the absence of forcing or dissipative terms. More detailed discussions of computational stability in connection with the present problem have been presented by Fischer (1959, 1965a), Platzman (1963), Kasahara (1965), and Gates (1968).

Having established that the non-diffusive terms in Equations (16-18) and (33-34) are to be evaluated at the central

time-step, it may still be advisable to use some form of centered differencing other than the leapfrog scheme for certain terms in the equations. Indeed almost all other time-extrapolation schemes applied in the field of meteorology and oceanography fit within the general framework of centered differencing even though the functions are approximated rather than evaluated at the centered time. In view of the usefulness of such procedures for the treatment of the Coriolis terms and the nonlinear terms, a brief review seems justified. For example, consider the basic equations (16-18) in the absence of forcing or dissipative terms and with the time derivatives replaced by centered differences.

$$\frac{1}{2\Delta t}\left[\, U(t+\Delta t) - U(t-\Delta t)\,\right] = -gH\,\frac{\partial \zeta(t^*)}{\partial x} + f\,V(t^*) - NL_x(t^*) \tag{67}$$

$$\frac{1}{2\Delta t}\left[\, V(t+\Delta t) - V(t-\Delta t)\,\right] = -gH\,\frac{\partial \zeta(t^*)}{\partial y} - f\,U(t^*) - NL_y(t^*) \tag{68}$$

$$\frac{1}{2\Delta t}\left[\, \zeta(t^*+2\Delta t) - \zeta(t^*)\,\right] = -\frac{\partial}{\partial x}\,U(t+\Delta t) - \frac{\partial}{\partial y}\,V(t+\Delta t) \tag{69}$$

where NL indicates the nonlinear acceleration terms and t^* is a dummy variable for the time t. The leapfrog scheme is obtained by replacing t^* by t, which represents the centered time for the U-V-field. The time lag between the equations of motion and the continuity equation assures that the pressure-gradient terms are available at the right time, but the Coriolis term and the nonlinear terms clearly call for a second prediction of the U-V-ζ -field with a time lag of one time step, so that the U-V-field will be available at time t and ζ becomes available at $t + \Delta t$.

With regard to the Coriolis terms this additional prediction can be eliminated by a time-interpolation of these terms. As discussed by Lilly (1961) this can be accomplished in two ways. The most accurate method is a treatment of the Coriolis terms by the familiar Euler-implicit or trapezoidal scheme. Thus the Coriolis terms are approximated as follows.

$$f\,V(t^*) \simeq \frac{1}{2}\,f\,[V(t-\Delta t) + V(t+\Delta t)]$$

$$f\,U(t^*) \simeq \frac{1}{2}\,f\,[U(t-\Delta t) + U(t+\Delta t)] \tag{70}$$

In this case the implicit character of the scheme causes no problems since the equations can be transformed immediately into explicit forms by solving the system of equations (67) and (68) in terms of the new velocity field. The second method suggested by Lilly (1961) is a combination of forward and backward differences where $t^* = t - \Delta t$ in the Coriolis term of equation (67) and $t^* = t + \Delta t$ in the Coriolis term of (68).

Another combination of forward and backward differences may be mentioned because it has been applied extensively in studies of storm surges in the North Sea (Fischer, 1959; Lauwerier, 1962; Heaps, 1969). Welander (1961) called this scheme the half-implicit scheme and it is essentially equivalent to the scheme obtained from (67-69) if t^* is replaced by $t-\Delta t$, which implies a forward differencing of the equations of motion and a backward evaluation of the continuity equation. With regard to the gravity waves this procedure is similar to the leapfrog scheme due to the special character of the equations (Fischer, 1965b). However, the forward differencing applied to the Coriolis terms introduces computational instability as pointed out by Fischer's (1959) stability analysis.

For the nonlinear terms in the equations (67-68) to be available at the centered time it appears necessary to carry along another prediction. As an alternative, the Euler implicit method can be applied to the complete equations (Uusitalo, 1960; Veronis, 1963) but its implicit character makes it very costly. If restricted to the first iterative approximation (Heun method) the most desirable properties of the scheme are lost. Another alternative for an additional leapfrog time extrapolation is found in prediction schemes of the Lax-Wendroff type where the nonlinear terms at time t are evaluated after a forward prediction from time $t-\Delta t$ to time t. In Phillips' (1960) case the forward step is Lagrangian, and other variations have been discussed by Fischer (1965a, 1965c) and Kasahara (1965). The schemes are known to have a damping effect on the high wave numbers but do not exhibit the computational or parasitic mode. Somewhat similar is the method of fractional time steps employed by Leith (1965) and consisting of a sequence of two Lagrangian steps. The first iterative approximation to the backward differencing (implicit) scheme used by Matsuno (1966) and Anthes (1970) results also in a damping of oscillatory solutions. The main problem remains that the computational effort is doubled whether an additional leapfrog prediction is carried along or any of the above substitutes is used. In addition, the evaluation of the nonlinear terms is time-consuming.

Extending the above to the three-dimensional model the following procedure is suggested for the prediction of the various parameters. Considering first the linear terms it can be seen from (31), (33), and (34) that it would be desirable for the variables ζ, D and T to be staggered in time with respect to U, V, and ω. Thus both the barotropic and baroclinic pressure gradients would be available at the centered time for the velocity computations, while the Coriolis term could be computed according to (70). Furthermore, the velocity components would be available at the centered time not only for the computation of the layer thicknesses from (31) but also for the nonlinear

temperature advection (39), which constitutes an essential part of the model. In the absence of the nonlinear inertial terms in the equations of motion it would then only remain to approximate the temperature at the time level of the velocity components for the purpose of computing the temperature advection, for instance by a Lax-Wendroff scheme. Again, however, the nonlinear terms in the equations of motion would essentially result in a doubling of the computational effort, and for many purposes it may be acceptable to drop these terms.

3.2 FINITE-DIFFERENCING IN SPACE

Turning now to the problem of space-differencing, the interior of the lake away from the shores will be considered first. There, a very natural and accurate method of replacing space derivatives by finite differences is to utilize centered differences in space. Considering the gravity waves described by the pressure and divergence terms, it is clear from the basic equations that the combination of central differences in time and space implies that the calculation of any one of the five variables U, V, T, D, ω requires a knowledge of the other variables at specific points in space and time. This leads to a certain disposition of the variables in time and space on the horizontal computational grid or lattice shown in Figure 3a, where ζ indicates a point where the surface elevation (ζ) and also the variables T, D, and ω are specified. The prime indicates a time lag of one time step with respect to the other variables. Notice that, whereas T, D, and ω are all defined in the ζ-points, only T and D are at the time level of ζ while ω is computed at the time level of the horizontal velocity components as

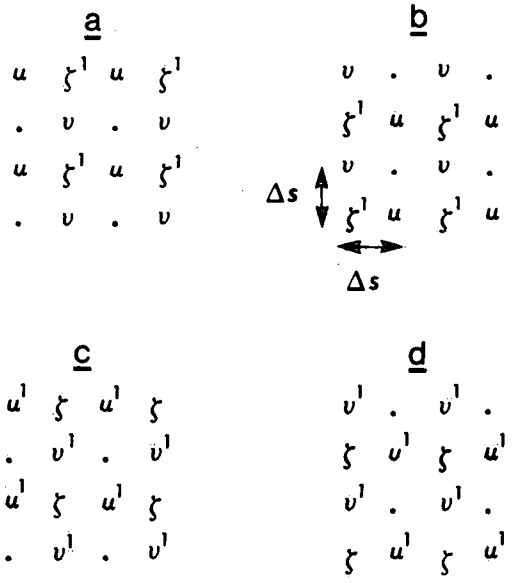

Figure 3. Finite difference lattices associated with centered differences in time and space. Primes denote time lag of one time step. *a*–basic lattice, *b*–space-supplement, *c*–time-supplement, *d*–conjugate lattice. Space location of variables D, T, and w in ζ-points, with w at time-level of velocity components.

indicated in the previous section. Although the basic grid of Figure 3a is in principle sufficient to perform the numerical calculations associated with the remaining terms of the equations, a proper modeling of the Coriolis forces and nonlinear terms is considerably simplified if at least one additional lattice is introduced. Possible alternatives are the space-supplement of the basic lattice shown in Figure 3b, the time-supplemental lattice shown in Figure 3c, or the space-time-supplement shown in Figure 3d, which is called the conjugate lattice in Platzman's (1963) notation.

Various combinations of the lattices *a*, *b*, *c*, and *d*, shown in Figure 3, can be considered with reference to the evaluation of non-frictional terms at centered time-steps and diffusive terms at previous time-steps. A direct evaluation of the Coriolis term without space interpolation calls for a definition of the U-components of the velocity at the V-points and vica versa. This can be accomplished by combining lattices *a* and *d* as proposed by Eliassen (1956) and Platzman (1963) or lattices *a* and *b* together with a time interpolation as suggested by Lilly (1961). As discussed before, this time extrapolation can be of two types, corresponding to a trapezoidal or a forward-backward differencing scheme,respectively. The latter was used by Sielecki (1968); the former was employed by Ueno (1964) and will be adopted for the present model of the Great Lakes.

A combination of lattices *a* and *c* does not add to the space resolution of the model and therefore necessitates a space interpolation of many terms of the equations including the Coriolis terms. The added time resolution is not of much value since the time step prescribed by the stability criterion (66) is already very small. On the other hand it is well known that the combinations *a* and *b* or *a* and *d* may result in semi-independent solutions on the individual lattices. This phenomenon is known as grid-dispersion and is essentially a measure of space truncation errors. The problem becomes most serious in natural basins with irregular bottom topography and shore configurations where each lattice is subject to different boundary conditions. It is true that the Coriolis term and the nonlinear terms call for a combination of lattices and consequently tend to couple the solutions on the individual lattices. This, however, is hardly desirable but should be regarded as a source of error and possibly computational instability. It is therefore most important to minimize the grid-dispersion in the absence of these terms. The most obvious technique of reducing the grid-dispersion consists of the application of space-smoothing operators (Shuman,1957). Such filters may be combined with finite-difference schemes as discussed in some detail by Harris and Jelesnianski (1964). However, a side-effect is the damping of oscillatory solutions which may be undesirable although it is mostly confined to the higher harmonics. It may be more satisfactory to accomplish a virtual smoothing by a proper modeling of the horizontal eddy diffusion of momentum. Thus, for the horizontal viscosity to couple the lattices *a* and *b* or the combination of *a* and *d*, the Laplace operator

should be evaluated by a rotation of the coordinate axes over 45 degrees.

A rotation of the coordinates may also be valuable for the evaluation of other space differences. This may be illustrated with the help of Figure 4, which shows two computational grids employed in preliminary test models. Each grid is composed of a least two lattices of the type shown in Figure 3. The mesh size of the second grid is smaller and the grid is rotated over 45 degrees. The higher resolution is irrelevant for purposes of the present discussion but the rotation is of interest. The basic coordinate system of model B is denoted by x'-y' in Figure 4B and the equations (16-18) are written for these rotated x'-y' coordinates. Finite differences are also evaluated along the rotated axes. It can be easily verified that, by adding and subtracting the equations of motion and relating the velocity components in the primed system to the original U-V-components, one would obtain a system of prediction equations of the type used by Lauwerier (1962), Leith (1965), and Heaps (1969), among others. The latter form of the equations would suggest a smoothing and a coupling of the lattices, and consequently a reduction of the grid-dispersion. Apparently, that is not the case, and any improvements resulting from this procedure (Lauwerier, 1962) must be traced to the orientation of the grid in relation to the boundaries of the basin. The effects of this orientation will be discussed in the last Section where computations on this grid are compared with results of model A. These numerical calculations have been performed in the primed coordinate system because the averaging appears to be an unnecessary computational effort.

The final aspect of the numerical procedure concerns the treatment of the lateral boundaries. The boundary condition for the velocity component normal to the shore can be incorporated readily if the computations are performed on a single lattice, e.g., lattice *a* in Figure 3. A virtual boundary can then be defined consisting of boundary segments parallel to either the x-axis or the y-axis, so that the segments parallel to the x-axis pass through points where V-values are located and segments in y-direction pass through U-points. The velocity components at boundary points are then set equal to zero. This technique was applied by Platzman (1958a) and also apparently by Hansen (1962), Henning (1962), and Rose (1962). If the computational grid consists of two basic lattices such as the grids shown in Figure 4, this method would result in two different virtual boundaries, one for each latice, which would cause a serious grid-dispersion problem (see, e.g., Sielecki, 1968). Furthermore, in such computational grids the boundaries will necessarily pass through elevation points or through points where the component of the velocity parallel to the boundary is defined. In that case the following procedures may be considered.

If an elevation point coincides with the boundary, the equation of continuity can be applied at such a point providing that forward space-differences are employed. This method assures conservation of mass and, as such, is equivalent to the condition that the velocity component normal to the wall must vanish. This method is equivalent to Platzman's (1963) boundary treatment and was used by Gates (1968). On the other hand, Harris and Jelesnianski (1964) suggested to obtain the gradient of the surface from the equation of motion perpendicular to the shore. The first method is employed in the present models in view of its desirable conservation properties.

The tangential velocity component at the shore can be obtained by applying the equation of motion for that component in a boundary point. This is the usual procedure in storm-surge studies (Fischer, 1959; Lauwerier, 1962; Platzman, 1963; Heaps, 1969). For boundary segments oriented with respect to the computational grid as in Figure 4A, the pressure-gradient term along the boundary can be evaluated immediately from boundary-elevation points. If

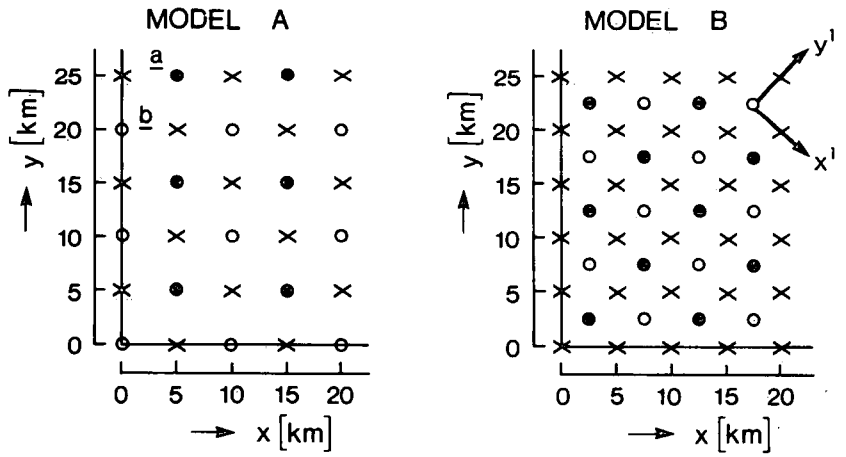

Figure 4. Computational grid employed in preliminary test models. Crosses denote stream points where both velocity components are specified. Circles indicate elevation points; open circles belong to lattice *b* (or *d*), black circles to lattice *a* of Figure 3.

the boundary segment is of the type shown in Figure 4B a special procedure is necessary to evaluate the pressure gradient in the equation of motion parallel to the shore. The following alternatives may be considered for the boundary points of model B.

The equations of motion in the x'- and y'-direction may be applied at a boundary streampoint by introducing a fictitious surface elevation at this boundary streampoint and evaluating the pressure gradients by forward differences (Sielecki, 1968). By adding and subtracting the equations and using the boundary condition for the velocity normal to the wall, one obtains a prediction equation for the tangential velocity. In the latter equation the pressure gradient along the wall is clearly replaced by the gradient along the first internal row of elevation points. For a more accurate evaluation of the pressure gradient at the wall, the surface elevations at the boundaries can be obtained by linear extrapolation of surface elevations computed at the first two rows of internal elevation points (Lauwerier, 1962). Heaps (1969) extended this method to a 3-point interpolation between two rows of interior and one row of fictitious exterior elevation points computed from the equation of motion perpendicular to the wall.

3.3 TREATMENT OF NONLINEAR TERMS

In the discussion of the energy conversions for a layered model, a major problem associated with space-differencing was touched upon, namely, the numerical treatment of nonlinear terms. A great deal of research has been devoted to this problem particularly after the introduction of numerical models in meteorology. The nonlinear processes tend to generate higher harmonics which cannot be dealt with effectively by the computational grid and which can lead to nonlinear computational instability as pointed out by Phillips (1959). An effective method to suppress higher harmonics is to introduce eddy diffusion or smoothing. Special numerical techniques have been proposed to deal with the problem of nonlinear instability, including the application of spectral techniques or the use of conservative finite-difference schemes. A review of various numerical schemes has recently been presented by Grammeltvedt (1969).

Many numerical schemes designed for the treatment of nonlinear terms are highly complicated and difficult to apply at the boundaries since a great number of grid points may be involved. In view of the character of the lateral boundaries in the present models it appears desirable to evaluate the nonlinear inertial terms in the equations of motion over not more than five adjacent stream points. This in turn calls for at least two lattices of the type shown in Figure 3, such as the double-lattice grids of Figure 4. Within the five-point restriction there are basically two alternatives. The first one is to average the variables along the x-axis of Figure 3a before evaluating the centered differences in the y-direction, and vice versa (e.g., Gates, 1968). The second method is to compute the components

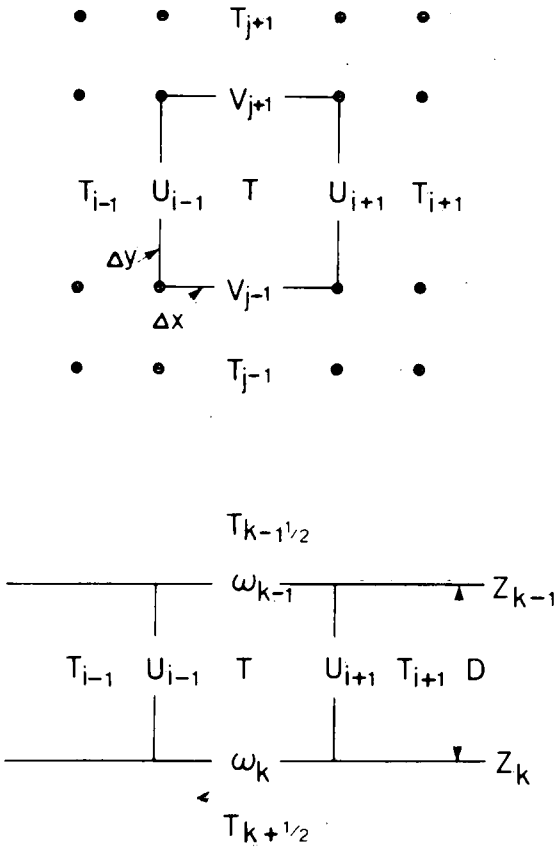

Figure 5. Typical horizontal (above) and vertical (below) staggering of variables in a layered model.

of the nonlinear inertial acceleration along the axis of a coordinate system rotated 45 degrees with respect to the main orientation of the grid. For example, whereas the main orientation of grid 4B is along the primed coordinates, the nonlinear terms could be evaluated along the unprimed axes. In the latter case one could average the variables along a given axis before taking centered differences along the same axis. The latter would be an example of a conservative scheme.

The principles of the energy-conserving finite-differencing procedure have been discussed by Arakawa (1968), Bryan (1966), and Lilly (1965). The purpose is to compute the nonlinear advection terms so that these terms do not affect the volume integrals of the advected quantity nor its variance. An outline of this method will now be presented for the type of equations under discussion. In particular the operator defined by (39) will be considered, which includes the corresponding one-layer operator as a special case. The discussion will be based on the disposition of variables shown in Figure 5, which corresponds to a horizontal lattice of the type of Figure 3 combined with the vertically layered system of Figure 2. It is understood that all subscripts are i, j, $k-\frac{1}{2}$, unless indicated otherwise, and that all variables are available at the same time. Furthermore, in each grid point only those variables have been entered which are called for in the

present discussion. In general, additional variables will be defined in the same grid points, and, conversely, the horizontal velocity components are not necessarily defined in the points indicated but may have to be obtained by interpolation. The latter could be the case in the computation of the nonlinear inertial terms.

For convenience the two equations (31) and (39) will be reproduced for a grid point with horizontal indices (i, j) and for the layer with index $k-\frac{1}{2}$. Dropping all indices unless they differ from the above

$$L(1) = \frac{\partial D}{\partial t} + \frac{\partial U}{\partial x} + \frac{\partial V}{\partial y} + \omega_{k-1} - \omega_k = 0 \qquad (71)$$

$$L(\theta) = \frac{\partial T}{\partial t} + \frac{\partial}{\partial x}\left(\frac{UT}{D}\right) + \frac{\partial}{\partial y}\left(\frac{VT}{D}\right) + (\omega\theta)_{k-1} - (\omega\theta)_k \qquad (72)$$

It will now be shown that the conservation requirements are satisfied if the values of the advected variables (in this case the temperature) on the surfaces of the box surrounding the point $[i, j, k-\frac{1}{2}]$ are approximated by simple linear interpolation. Further, replacing the derivatives by ordinary centered differences, the equations above become

$$L(1) = \frac{\partial D}{\partial t} + \frac{1}{\Delta x}(U_{i+1} - U_{i-1}) + \frac{1}{\Delta y}(V_{j+1} - V_{j-1}) + \omega_{k-1} - \omega_k = 0 \qquad (73)$$

$$L(\theta) = \frac{\partial T}{\partial t} + \frac{U_{i+1}}{2\Delta x}\left[\frac{T}{D} + \left(\frac{T}{D}\right)_{i+1}\right] - \frac{U_{i-1}}{2\Delta y}\left[\frac{T}{D} + \left(\frac{T}{D}\right)_{i-1}\right] + \frac{V_{j+1}}{2\Delta y}\left[\frac{T}{D} + \left(\frac{T}{D}\right)_{j+1}\right] - \frac{V_{i-1}}{2\Delta y}\left[\frac{T}{D} + \left(\frac{T}{D}\right)_{j-1}\right] + \frac{1}{2}\omega_{k-1}\left[\frac{T}{D} + \left(\frac{T}{D}\right)_{k-\frac{3}{2}}\right] - \frac{1}{2}\omega_k\left[\frac{T}{D} + \left(\frac{T}{D}\right)_{k+\frac{1}{2}}\right] \qquad (74)$$

It follows that the summation of (73) or (74) over all layers and all grid points reduces to the summation of the first terms on the right-hand sides by virtue of the cancellation of all other terms, together with the boundary conditions on (U, V) and ω which vanish at the proper boundaries. Thus the volume integral of θ is not affected by the nonlinear advection terms. Obviously this property of (74) is not lost if (73) is substituted in (74) with the result

$$L(\theta) = \frac{\partial T}{\partial t} + \frac{T}{2D}\frac{\partial D}{\partial t} + \frac{1}{2\Delta x}\left[\left(\frac{UT}{D}\right)_{i+1} - \left(\frac{UT}{D}\right)_{i-1}\right] + \frac{1}{2\Delta y}\left[\left(\frac{VT}{D}\right)_{j+1} - \left(\frac{VT}{D}\right)_{j-1}\right] + \frac{1}{2}\left[\omega_{k-1}\left(\frac{T}{D}\right)_{k-\frac{3}{2}} - \omega_k\left(\frac{T}{D}\right)_{k+\frac{1}{2}}\right] \qquad (75)$$

If the latter is multiplied by T/D then

$$\frac{T}{D}L(\theta) = \frac{\partial}{\partial t}\left(\frac{T^2}{2D}\right) + \frac{1}{2\Delta x}\left[U_{i+1}\left(\frac{T}{D}\right)_I\left(\frac{T}{D}\right)_{i+1} - U_{i-1}\left(\frac{T}{D}\right)_{i-1}\left(\frac{T}{D}\right)_I\right] + \frac{1}{2\Delta y}\left[V_{j+1}\left(\frac{T}{D}\right)_J\left(\frac{T}{D}\right)_{j+1} - V_{j-1}\left(\frac{T}{D}\right)_{j-1}\left(\frac{T}{D}\right)_J\right] + \frac{1}{2}\left[\omega_{k-1}\left(\frac{T}{D}\right)_{k-\frac{3}{2}}\left(\frac{T}{D}\right)_{k-\frac{1}{2}} - \omega_k\left(\frac{T}{D}\right)_{k+\frac{1}{2}}\left(\frac{T}{D}\right)_{k-\frac{1}{2}}\right] \qquad (76)$$

Again the summation of (76) over all points reduces to the summation of the first term on the right by virtue of the same cancellation effects and boundary conditions mentioned below (74). This first term is just the time rate of change of $\theta^2/2$ for a layer, according to (37), and hence the volume integral is not affected by the nonlinear advection terms. Consequently, the scheme is conservative in the sense defined above. With regard to the layered representation in the vertical, a similar argument was presented already in the framework of the energy considerations.

In summary it is concluded that the advection of a given variable is to be computed by surrounding the grid point by a box as illustrated in Figure 5, using a linear interpolation for the advected variable on the surfaces of the box, and requiring that the advecting velocities on these surfaces be related to each other by (73). It is clear from the above that the values of the advecting velocities U, V, ω at the surfaces of the box do not have to be grid point values, as mentioned before. These velocity components may be obtained by interpolation if for reasons of other computations it is more convenient to define one or more of these variables at grid points different from those shown in Figure 5. This is the case if one wants to compute the

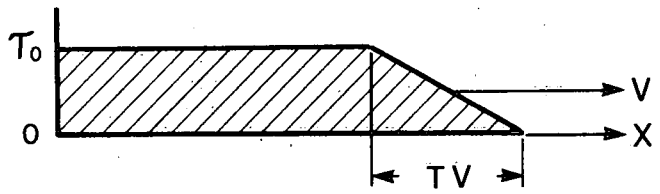

Figure 6. Idealized wind field simulating the passage of an atmospheric front.

nonlinear terms in the equations of motion, where one is dealing with a box surrounding a velocity point. In that case, the condition that the velocity components must be mutually consistent in the sense that (73) is to be satisfied, leads to a computation of ω in points which lie immediately above and below the velocity points. Since the temperature calculation already calls for ω in the elevation points, this results in a doubling of ω-points.

3.4 ONE-DIMENSIONAL TEST COMPUTATIONS

Before proceeding to more realistic models of the Great Lakes it is useful to consider the response of simple lake models to time-dependent wind stresses. If the situation considered is simple enough, it may be possible to obtain analytical solutions which not only give us an idea of the behaviour of the physical system but also can be used to test the numerical solutions. For example, in the case of Lake Ontario one is dealing with a lake of considerably smaller size than the scales of atmospheric disturbances. The lake has a narrow elongated shape, it is situated in the belt of atmospheric westerlies, and its main axis is nearly parallel to the prevailing wind direction. It is thus of interest to consider the problem of a time-dependent wind field of large space dimensions blowing along the length axis of an elongated rectangular homogeneous basin, ignoring as a first approximation the effects of the earth's rotation, the nonlinear effects, and the eddy diffusion. At first it will also be assumed that the depth is uniform in which case this wind stress will not generate any transverse motions and the problem becomes effectively one-dimensional.

Considering the general behaviour of the wind following the passage of a front, the wind tends to increase sharply for a relatively short period of time, say T, and thereafter varies more slowly. At the same time the wind field will move across the lake in the general direction of the wind stress. Idealizing this situation we consider a semi-infinite stress band with a linear increase of intensity over a period of time, T, and a constant intensity after time T, and moving with a constant translation speed V. This wind field is shown in Figure 6, where τ_0 is the scale value of the stress. Notice that the setup for a finite stress band may be obtained by superposition of two semi-infinite stress bands, a positive stress and a negative stress of the same intensity, moving in the same direction, but separated by a time lag. Notice also that the linear increase of stress implies a wind increase proportional to the square root of time.

The present problem has been solved by Rao (1967) for a step-function wind stress (T=0) using the method of characteristics. As the same technique will be applied here no detailed discussion of the procedure is presented. Consider a lake of uniform width, W, uniform depth, H, finite length, L, and let the x-axis be oriented along the length axis of the lake. Without the Coriolis terms, the nonlinear effects, and the frictional terms, the one-dimensional equations corresponding to (16-18) are

$$\frac{\partial U}{\partial t} = -gH\frac{\partial \zeta}{\partial x} + \frac{\tau_s}{\rho}; \quad \frac{\partial \zeta}{\partial t} = -\frac{\partial U}{\partial x} \tag{77}$$

where the time-dependent windstress at the surface (τ_s) is of the form shown in Figure 6, and the front is taken to arrive at the left end of the lake (x=0) at time t=0. The boundary conditions are then U=0 at x=0 and x=L, and the initial conditions are U=ζ=0 at t=0. Let c=$\sqrt{gH}$ be the speed of the free gravity wave and introduce the non-dimensional quantities

$$x' \equiv x/L, \quad t' \equiv ct/L, \quad v' \equiv V/c, \quad T' \equiv cT/L$$
$$\tau_s' \equiv \tau_s/\tau_0, \quad \zeta' \equiv \rho c^2\zeta/\tau_0 L, \quad U' \equiv \rho cU/\tau_0 L \tag{78}$$

where τ_0 is the scale value of the wind stress (Fig. 6). Upon adding and subtracting the nondimensional forms of equation (77) it follows that

$$\frac{d}{dt'}(U' \pm \zeta') = \tau_s' \quad \text{for} \quad \frac{dx'}{dt'} = \pm 1 \tag{79}$$

These equations can be integrated easily in the x', t'-plane along the straight characteristics x=± t + constant, noting that

$$\begin{aligned} \tau_s' &= 0 && \text{for } x' > V't' \\ \tau_s' &= 1 && \text{for } x' < V'(t' - T') \\ \tau_s' &= \left(t' - \frac{x'}{V'}\right)/T' && \text{for } V'(t'-T') < x' < V't' \end{aligned} \tag{80}$$

The speed of the free gravity wave for Lake Ontario is of the order of 30 m/sec. As this velocity is never attained by moving atmospheric disturbances, we may restrict ourselves to the case $V' \equiv V/c < 1$.

The solutions for this case are summarized in Table 1, where ζ_0 is the surface elevation at the left end of the basin (x=0) and ζ_1 is the elevation at the other end (x=L). All variables in the table are nondimensional, but for convenience the primes have been dropped. Furthermore, min (α,β) denotes the smallest of the two numbers α and β and max (α,β) indicates the larger of the two. As an example of the solutions of Table 1, the response of the lake to a few typical stress bands is shown in Figure 7. For comparison with Lake Ontario, dimensional numbers based on the values c=32 m/s, L=300 km, and τ_0/ρ = 1 cm^2/s^2 have been included, thus V=32 V' (m/s), T=2.6T' (hr), ζ=2.91 ζ' (cm),

TABLE 1. One-dimensional response of a lake to the idealized wind shown in Figure 6.

Definitions

$A_0 \equiv \left[2T\left(\frac{1}{V}+1\right)\right]^{-1}$	$A_1 \equiv \left[2T\left(\frac{1}{V}-1\right)\right]^{-1}$
$B_0 \equiv \min\left(T, \frac{1}{V}+1\right)$	$B_1 \equiv \min\left(T, \frac{1}{V}-1\right)$
$C_0 \equiv \max\left(T, \frac{1}{V}+1\right)$	$C_1 \equiv \max\left(T, \frac{1}{V}-1\right)$
$D_0 \equiv T + \frac{1}{V}+1$	$D_1 \equiv T + \frac{1}{V}-1$

Solutions

time	$\zeta_0(t) - \zeta_1(t\text{-}1)$	time	$\zeta_1(t+1) - \zeta_1(t)$
$t<0$	0.	$t<0$	0.
$0<t<B_0$	$-A_0 t^2$	$0<t<B_1$	$A_1 t^2$
$B_0<t<C_0$	$-A_0B_0(2t-B_0)$	$B_1<t<C_1$	$A_1B_1(2t-B_1)$
$C_0<t<D_0$	$-1+A_0(t-D_0)^2$	$C_1<t<D_1$	$1-A_1(t-D_1)^2$
$D_0<t$	-1	$D_1<t$	1.

and $t=2.6t'$ (hr). These and many other cases were also computed by the numerical techniques discussed earlier, that is, centered differences in space and time. Comparison of the exact and the numerical solutions indicated that the truncation error with a gridmesh of 5 km is less than 1%.

The character of the solutions above is important and a brief discussion therefore may be inserted here. The present solutions are similar to Rao's (1967) results for T=0 except for the somewhat smoother response of the lake as seen from Figure 7. It follows from Table 1 that ζ_0 is periodic for $t' > T' + \frac{1}{V'} + 1$ and ζ_1 is periodic for $t' > T' + \frac{1}{V'} + 2$ with period $\Delta t'=2$ or $\Delta t=2L/c$. In Rao's special case (T=0) the surface elevations ζ_0 and ζ_1 approach the constant values $\zeta_0' = -\frac{1}{2}$, $\zeta_1' = \frac{1}{2}$, for $V' = 1/(2n+1)$ where n is a positive integer. Another special case which may be considered is the wind stress associated with a deepening storm situated over the lake. The solution can be obtained from the general solution by letting V' approach infinity but the solutions for $V' > 1$ have not been included in Table 1. If this special case was solved, it would be found that the response approaches the constant values $\zeta_0' = -\frac{1}{2}$, $\zeta_1' = \frac{1}{2}$, if $T'=2n$ where n is a positive integer. From simple considerations it may then be concluded that the general solutions of Table 1 approach a

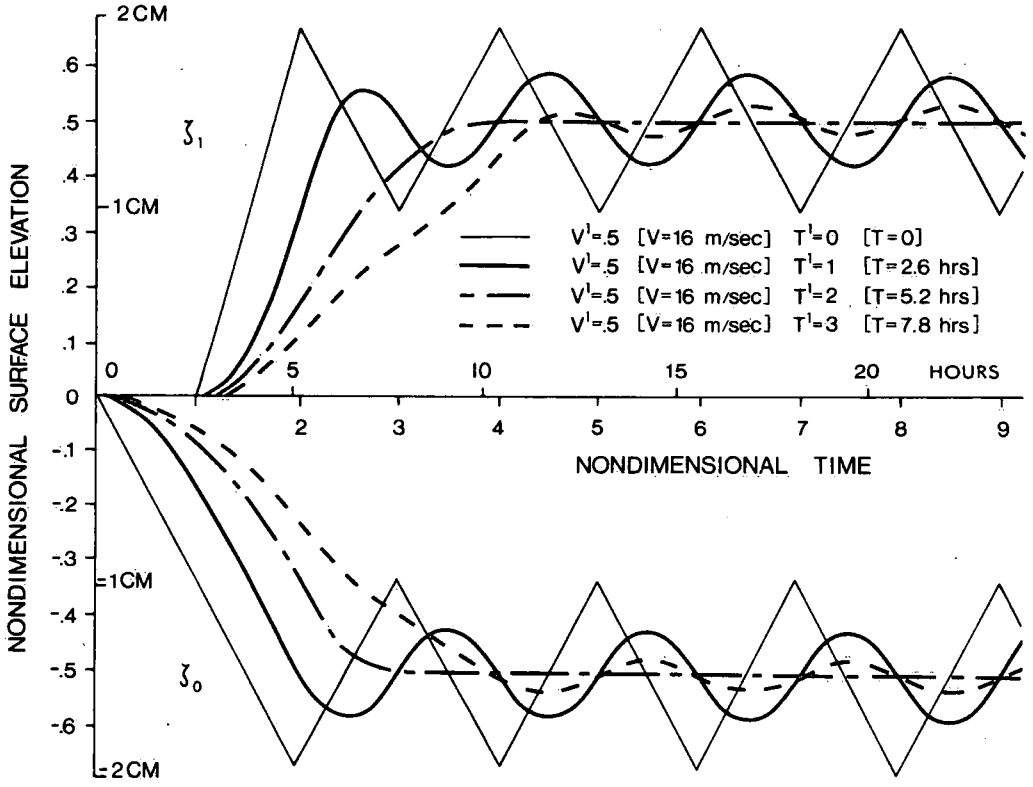

Figure 7. One-dimensional response of a lake to a wind field of the type shown in Figure 6. Dimensional quantities based on unit wind stress and dimensions of Lake Ontario.

non-oscillatory, steady state for V'=1/(2n+1) or T'=2n. This is of particular interest if we consider an idealized wind field with a velocity V=10 m/s and a period of intensification equal to T=5 hr, which appear to be fairly reasonable values. Using the same representative values for Lake Ontario given above we find V'=1/3 and T'=2 (approximately). Each of these values tends to favour a steady set up.

3.5 TWO-DIMENSIONAL TEST COMPUTATIONS

Returning now to the numerical aspects of the problem a two-dimensional extension of the above solution is considered. The response of the rectangular lake to the same wind is computed with the same assumptions introduced earlier except for the following. The depth is now taken to vary in the direction perpendicular to the wind which tends to induce transverse motions and consequently we are dealing with a two-dimensional problem. As before, the only terms retained for the moment in Equations (16-18) are the pressure gradients, the divergence terms, and the wind stress.

The length of the rectangular basin is 300 km and the cross-section corresponds to the depth profile of Lake Ontario at longitude 78°W. Thus the width of the model is 70 km and the average depth is 105 m as denoted by the dashed line in Figure 8. The corresponding velocity of the free surface wave is about 32 m/s, which was used above for conversion from non-dimensional to dimensional quantities. The x-axis is taken along the length-axis pointing eastward and the y-axis points northward. The wind blows again along the x-axis and consequently the response of the basin without depth variations would be the same as the one-dimensional response above. The computational grids have been discussed in connection with Figure 4. Each grid is composed of the lattices *a* and *b* shown in Figure 3. To identify the lattices, the elevation points belonging to lattice *a* are denoted by black circles while open circles indicate the elevation points of lattice *b*. The distance between grid points is 5 km for grid A of Figure 4 and $5/\sqrt{2}$ km for grid B. Centered differences in time and space are used except for the boundary-elevation points where the divergence is evaluated by forward space-differences. The normal velocity is zero at the wall and the tangential velocity is either computed from the equation of motion parallel to the wall or set equal to zero.

As noted before, the utilization of centered differences in time and space in the present model implies the existence of two independent solutions on lattice *a* and *b* respectively. In model A of Figure 4 each lattice is subject to computationally different boundary conditions. For lattice *a* (black circles) the condition is that the normal velocity component vanish at the boundary, for lattice *b* (open circles) the same condition prevails but the normal component of the velocity is not specified at the wall. Instead, the condition is satisfied by a proper computation of the divergence in the boundary points. In order to assure that these conditions are compatible, the solutions on the two lattices are compared for the case of uniform depth and found in perfect agreement. For comparison with the exact solutions described above the surface elevation at the boundary for lattice *a* is obtained by a linear extrapolation from the first two interior points of the same lattice. The exact solutions are well approximated by both lattices; in fact, the errors do not exceed one percent of the true solution.

Consider now the depth profile of Figure 8, where we let the depth at the shores approach a small but non-zero value, H = 1 m. Clearly the bottom profile affects the two lattices of model A in different ways, and in particular the shallow depths at the shores are perceived by lattice *b* only. The upper part of Figure 9 shows the response of the basin to a wind impulse given by $\tau_s = 0$ for $t < 0$ and $\tau_s/\rho = 1$ cm^2/s^2 for $t > 0$. The dashed curve is the response of model A at x = 0, y = 25 km, that is, grid *a*. The dot-dash curve is the response at point x=0, y=20 km belonging to grid *b*. By comparison with neighboring points it is found that the surface elevations at distances of 10 km along the boundary are nearly the same. Hence the differences between the two curves are caused almost entirely by grid dispersion. The considerable dispersion is mostly induced by the shallow depths at the shores which tend to retard the oscillations of the solution on lattice *b* since the free surface wave moves very slowly in this shallow water.

In the present case the grid dispersion can be related immediately to the orientation of the grid with respect to the bottom contours and lateral boundaries. Rotation of the computational grid as shown in Figure 4B is therefore indicated. The computational procedure has been described earlier. Thus the x, y-coordinate system is

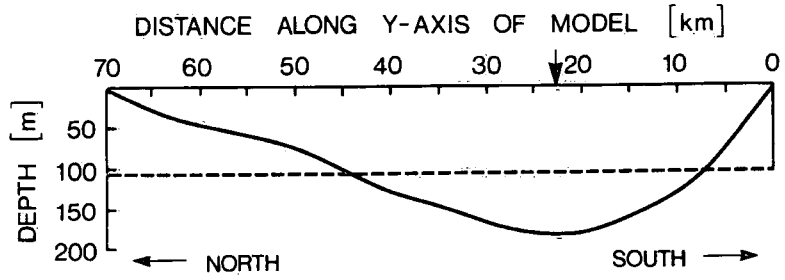

Figure 8. Depth profile of Lake Ontario at longitude 78°W, employed in studies or rectangular basin.

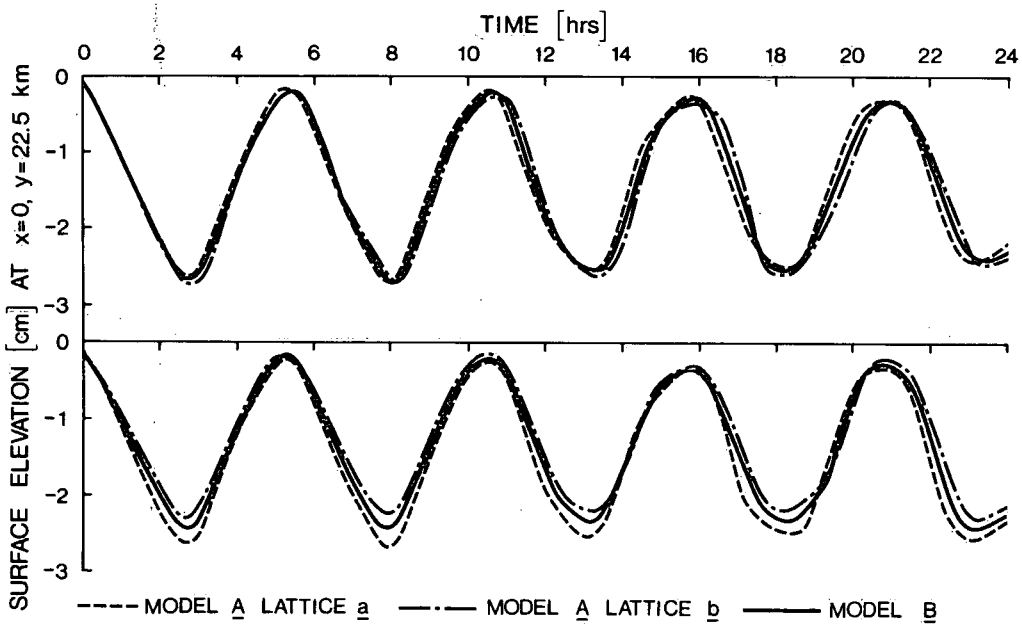

Figure 9. Response of rectangular basin to wind inpulse of unit stress, measured at location of arrow in Figure 8. Upper part of figure for free-slip walls, lower part for no-slip walls.

replaced by the primed system as the basic coordinates for the calculations at interior points. The pressure gradients along the wall necessary for the prediction of the tangential velocity component in the case of free-slip boundaries are obtained by linear extrapolation from the first two internal points. Integrations with model B show indeed that the grid dispersion is completely suppressed for the present bottom configuration. The solid line in the upper part of Figure 9 shows the response of model B to the same wind stress imposed on model A. The surface elevation shown corresponds to the point x=0, y=22.5 km. On the scale of Figure 9 the latter coincides with the response at x=0, y=27.5 km which means that the grid dispersion has been eliminated. As expected, the solid line is a weighted average of the dashed line and the dot-dash curve.

The same experiments may now be repeated with the boundary condition that both components of the transport vector vanish at the shore. The results are shown in the lower part of Figure 9. The dashed curve shows the response of lattice *a* of model A which is not affected by the new boundary condition and consequently this curve is the same as before. The dot-dash line shows the response of lattice *b* of model A and the solid line indicates again the response of model B which is once more free of grid dispersion. The general behavior of the solutions for free-slip boundaries and for no-slip walls is similar in that the presence of the boundaries in either case tends to slow down the oscillations. In addition, the no-slip boundary tends to reduce the amplitude of the oscillation. Since the oscillation of the basin is the integrated effect of the oscillations of a number of channels of various depths, a large contribution to the total amplitude comes from the shallow shores. This contribution is annihilated by the condition of no-slip boundaries. If the same computations are performed for a channel of constant depth, the amplitudes of the solutions are the same for each lattice and each model. However, the no-slip boundary condition results in an increase of the period of oscillation on grid *b* of model A equal to about 7% by comparison to solution *a* of model A. This could be expected since there are 14 grid intervals in the transverse direction. In this case the period of oscillation of model B is increased by 3-4%, again without grid dispersion.

Although the no-slip boundaries appear to cause a larger grid dispersion than the free-slip boundaries, it is believed that the former boundary condition represents a reasonable simulation of the retarding effect exerted on the large-scale flow by the lateral boundaries. Thus this condition is adopted for the present models in conjunction with the effects of horizontal eddy diffusion. The lateral boundary layer introduced by this procedure has an effective width equal to the grid distance. In the present models this is of the order of 5 km, which probably underestimates the nearshore velocities. An improvement may be achieved by a quadratic interpolation of the velocities for the purpose of computing the divergence in the first internal row of elevation points of model B, or by using a finer grid at the boundaries. Some preliminary computations have been performed to study the effects of such refinements. As expected, the results are weighted averages of the free-slip and the no-slip-boundary solutions shown in Figure 9. It is found, however, that weak instabilities may be introduced by such procedures. Although this could be related to a coupling of the lattices (Platzman, 1958b), it should be noted that such coupling occurs always at the boundaries of model B in the case of free-slip walls.

References

Anthes, R. A. 1970. Numerical Experiments with a Two-Dimensional Horizontal Variable Grid. Mon. Weath. Rev., 98, 810-822.

Arakawa, A. 1966. Computational Design for Long-Term Numerical Integration of the Equations of Fluid Motion: I. Two-Dimensional Incompressible Flow. J. Comput. Physics, 1, 119-143.

Baer, F. and T. J. Simons, 1970. Computational Stability and Time Truncation of Coupled Nonlinear Equations with Exact Solutions. Mon. Weath. Rev., 98, 665-679.

Bryan, K. 1963. A numerical Investigation of a Non-Linear Model of a Wind-Driven Ocean. J. Atmos. Sci., 20, 594-606

Bryan, K. 1966. A Scheme for Numerical Integration of the Equations of Motion on an Irregular Grid free of Nonlinear Instability. Mon. Weath. Rev., 94, 39-40.

Bryan, K. 1969. A Numerical Method for the Study of Ocean Circulation. J. Computat. Phys. 4, 347-376.

Bryan, K. and M. D. Cox, 1967. A Numerical Investigation of the Oceanic General Circulation. Tellus 19, 54-80.

Bryan, K. and M. D. Cox, 1968. A Nonlinear Model of an Ocean Driven by Wind and Differential Heating: part I and II. J. Atmos. Sci., 25, 945-978.

Cox, M. D. 1970. A Mathematical Model of the Indian Ocean. Deep-Sea Research, 17, 47-75.

Crowley, W. P. 1968. A Global Numerical Ocean Model: Part I. J. Computat. Phys., 3, 111-147.

Csanady, G. T. 1967. Large-Scale Motion in the Great Lakes. J. Geophys. Res., 72, 4151-4162.

Csanady, G. T. 1968a. Wind-Driven Summer Circulation in the Great Lakes. J. Geophys. Res., 73, 2579-2589.

Csanady, G. T. 1968b. Motions in a Model Great Lake Due to a Suddenly Imposed Wind. J. Geophys. Res. 73, 6435-6447.

Eliassen, A. 1956. A Procedure for Numerical Integration of the Primitive Equations of the Two-Parameter Model of the Atmosphere. Sci. Rept. No 4, Dept. of Meteorology, UCLA, 53 pp.

Fischer, G. 1959. Ein Numerisches Verfahren zur Errechnung von Windstau und Gezeiten in Randmeeren. Tellus, 11, 60-76.

Fischer, G. 1965a. A Survey of Finite-Difference Approximations to the Primitive Equations. Mon. Weath. Rev., 93, 1-10

Fischer, G. 1965b. Comments on "Some Problems Involved in the Numerical Solutions of Tidal Hydraulics Equations". Mon. Weath. Rev., 93, 110-111.

Fischer, G. 1965c. On a Finite-Difference Scheme for Solving the Nonlinear Primitive Equations for a Barotropic Fluid with Application to the Boundary Current Problem. Tellus, 17, 405-412.

Gates, W. L. 1968. A Numerical Study of Transient Rossby Waves in a Wind-Driven Homogeneous Ocean. J. Atmos. Sci., 25, 3-22.

Gates, W. L. 1970. Effects of Western Coastal Orientation on Rossby-Wave Reflection and the Resulting Large-Scale Oceanic Circulation. J. Geophys. Res., 75, 4105-4120.

Grammeltvedt, A. 1969. A Survey of Finite-Difference Schemes for the Primitive Equations for a Barotropic Fluid. Mon. Weath. Rev., 97, 384-404.

Hansen, W. 1956. Theorie zur Errechnung des Wasserstandes und der Strömungen in Randmeeren nebst Anwendungen. Tellus, 8, 287-300.

Hansen, W. 1962. Hydrodynamical Methods Applied to Oceanographic Problems. Proc. Symp. Math. Hydrodyn. Methods Phys. Oceanography. Univ. of Hamburg, 25-34.

Harris, D. L. and C. P. Jelesnianski. 1964. Some Problems Involved in the Numerical Solutions of Tidal Hydraulics Equations. Mon. Wea. Rev., 92, 409-422.

Heaps, N. S. 1969. A Two-Dimensional Numerical Sea Model. Philos. Trans. Roy. Soc. London, Series A, 265, 93-137.

Henning, D. 1962. Computation of a Storm Surge in the Baltic Sea. Proc. Symp. Math-Hydrodyn. Methods of Phys. Oceanography, Univ. of Hamburg, 257-263.

Jelesnianski, C. P. 1967. Numerical Computations of Storm Surges with Bottom Stress. Mon. Weath. Rev., 95, 740-756.

Jelesnianski, C. P. 1970. Bottom-Stress Time-History in Linearized Equations of Motion for Storm Surges. Mon. Weath. Rev., 98, 462-478.

Kasahara, A. 1965. On Certain Finite-Difference Methods for Fluid Dynamics. Mon. Weath. Rev., 93, 27-31.

Kurihara, Y. 1965. On the Use of Implicit and Iterative Methods for the Time Integration of the Wave Equation. Mon. Weath. Rev., 93, 33-46.

Lauwerier, H. A. 1962. Some Recent Work of the Amsterdam Mathematical Centre on the Hydrodynamics of the North Sea. Proc. Symp. Math-Hydrodyn. Methods Phys. Oceanography, Hamburg Univ., 13-24.

Lee, K. K., and J. A. Liggett. 1970. Computation for Circulation in Stratified Lakes. J. Hydraul. Div., ASCE, 96, 2089-2115.

Leith, C. E. 1965. Numerical Simulation of the Earth's Atmosphere. Methods in Comput. Phys, 4, 1-28.

Lilly, D. K. 1961. A Proposed Staggered-Grid System for Numerical Integration of Dynamic Equations. Mon. Weath. Rev., 89, 59-65.

Lilly, D. K. 1965. On the Computational Stability of Numerical Solutions of Time-Dependent Non-Linear Geophysical Fluid Dynamics Problems. Mon. Weath. Rev., 93, 11-26.

Lilly, D. K. 1967. The Representation of Small-Scale Turbulence in Numerical Simulation Experiments. Proc. IBM Sci. Comp. Symp. on Environmental Sciences, IBM Form No 320-1951, 195-210 .

Matsuno, T. 1966. Numerical Integrations of the Primitive Equations by a Simulated Backward Difference Method. J. Meteor. Soc. Japan, Ser. 2, 44, 76-84.

Miyazaki, M., T. Ueno, S. Unoki, 1961. Theoretical Investigation of Typhoon Surges along the Japanese Coast. I. Ocean. Mag, 13, 51-75; II Ocean. Mag., 13, 103-117.

Paskausky, D. F. 1969. A Barotropic Prognostic Numerical Model of the Circulation in the Gulf of Mexico. Dept. of Phys. Oceanography, Texas A M Univ.

Phillips, N. A. 1959. An Example of Non-Linear Computational Instability. The Atmosphere and Sea in Motion, Rockefeller Institute Press, New York, 501-504.

Phillips, N. A. 1960. Numerical Weather Prediction. Advances in Computers, 1, 43-90.

Phillips, N. A. 1962. Numerical Integration of the Hydrostatic System of Equations with a Modified Version of the Eliassen Finite-Difference Grid. Proc. Int'1. Symp. Num. Weath. Pred., Tokyo 1960, 109-120.

Platzman, G. W. 1958a. A Numerical Computation of the Surge of 26 June 1954 on Lake Michigan. Geophysica 6, 407-438

Platzman, G. W. 1958b. The Lattice Structure of the Finite-Difference Primitive and Vorticity Equations. Mon. Weath. Rev., 86, 285-292.

Platzman, G. W. 1963. The Dynamic Prediction of Wind Tides on Lake Erie. Meteor. Monog., 4, No 26, 44 pp.

Platzman, G. W. 1965. The Prediction of Surges in the Southern Basin of Lake Michigan. Part I: The Dynamical Basis for Prediction. Mon. Weath. Rev. 93, 275-281.

Rao, D. B. 1967. Response of a Lake to a Time-Dependent Wind Stress. J. Geophys. Res. 72, 1697-1708.

Rao, D. B. and T. S. Murty. 1970. Calculation of the Steady State Wind-Driven Circulations in Lake Ontario. Arch. Met. Geophys. Bioklim. Ser. A, 19, 195-210

Rose, D. 1962. The Influence of the Closed Sea-Arms on the Water Level and Current off the Coast of the Netherlands and in the New Waterway. Proc. Symp Math.-Hydrodyn. Methods Phys. Oceanography, Hamburg Univ., 227-231

Shuman, F. G. 1957. Numerical Methods in Weather Prediction. II. Smoothing and Filtering. Mon. Weath. Rev., 85, 357-361.

Shuman, F. G. and J. B. Hovermale, 1968. An Operational Six-Layer Primitive Equation Model. J. Appl. Meteor., 7, 525-547.

Sielecki, A. 1968. An Energy-Conserving Difference Scheme for the Storm Surge Equations. Mon. Weath. Rev. 96, 150-156.

Simons, T. J. 1971. Development of Numerical Models of Lake Ontario. Proc. 14th Conf. Great Lakes Res., 654-669.

Simons, T. J. 1972. Development of Numerical Models of Lake Ontario, Part 2. Proc. 15th Conf. Great Lakes Res., 655-672.

Smagorinsky, J., S. Manabe, and J.L. Holloway, Jr., 1965. Numerical Results from a Nine-Level General Circulation Model of the Atmosphere. Mon. Weath. Rev. 93, 727-768.

Ueno, T. 1964. Non-Linear Numerical Studies on Tides and Surges in the Central Part of Seto Inland Sea. Ocean, Mag., 16, 53-124.

Uusitalo, S. 1960. The Numerical Calculation of Wind Effect on Sea Level Elevations. Tellus, 12, 427-435.

Veronis, G. 1963. An Analysis of Wind-Driven Ocean Circulation with a Limited Number of Fourier Components. J. Atmos. Sci., 20, 577-593.

Veronis, G. 1966. Wind-Driven Ocean Circulation—Part 2: Numerical Solutions of the Non-Linear Problem. Deep-Sea Res., 13, 31-56.

Welander, P. 1961. Numerical Prediction of Storm Surges. Advances in Geophysics, 8, 315-379.

Welander, P. 1968. Wind-Driven Circulation in One-and Two-Layer Oceans of Variable Depth. Tellus, 20, 1-15.

Young, J. A. 1968. Comparative Properties of Some Time Differencing Schemes for Linear and Nonlinear Oscillations. Mon. Weath. Rev., 96, 357-364.

Yuen, K. 1968. A Numerical Study of Large Scale Motions in a Two-Layer Rectangular Basin under the Influence of Wind Stress. Marine Sciences Branch, Dept. of EMR, Ottawa, Canada, Manuscript Report Series No. 14.